The potential of lignocellulosic biomass precursors for biochar production: Performance, mechanism and wastewater application—A review

Article *in* Industrial Crops and Products · February 2019

DOI: 10.1016/j.indcrop.2018.11.041

CITATIONS
240

READS
335

2 authors:

Rangabhashiyam S
SRM University-AP, Amaravati, Andhra Pradesh, 522240, India
182 PUBLICATIONS **5,630** CITATIONS
SEE PROFILE

Balasubramanian Paramasivan
National Institute of Technology Rourkela
151 PUBLICATIONS **3,520** CITATIONS
SEE PROFILE

Industrial Crops & Products 128 (2019) 405–423

Contents lists available at ScienceDirect

Industrial Crops & Products

journal homepage: www.elsevier.com/locate/indcrop

The potential of lignocellulosic biomass precursors for biochar production: Performance, mechanism and wastewater application—A review

Rangabhashiyam. S[a,*], Balasubramanian. P[b,*]

[a] School of Chemical and Biotechnology, SASTRA University, Thanjavur, 613401, Tamilnadu, India
[b] Department of Biotechnology and Medical Engineering, National Institute of Technology Rourkela, Odisha, 769 008, India

ARTICLE INFO

Keywords:
Lignocellulosic biomass
Pyrolysis
Biochar
Adsorption
Heavy metals
Dyes

ABSTRACT

The organic and inorganic pollutants in water stream are due to the various industrial activities, consequent to the higher level environmental contamination. Considering the high toxicity and persistent property of wastewater pollutants, sequestration before discharge into water bodies becomes an important obligation. The conventional treatment methods are mostly associated with the drawbacks of energy intensive conditions and require high investment. Biochar produced through thermal decomposition of lignocellulosic biomass in the limited oxygen conditions offer as the sustainable potential adsorbent towards wastewater pollutants removal. The current review discusses on the utilization of various lignocellulosic biomass precursor for the production of biochar. The significant parameter influence and mechanistic aspects of the biochar production using pyrolysis were critically analyzed. The recent research on biochar modifications through different physical and chemical methods to enhance biochar adsorption property was reported. The new trend of the potential application of biochar in the adsorption of heavy metals, dyes and the underlying mechanisms are comprehensively reviewed. Further explorations are required in the directions of sustainable biochar development, continuous adsorption process, industry scale applications and spent biochar management.

1. Introduction

Water is one of the most important crucial molecules for life. In the present world, there is a growing concern about the improvement of water quality and its preservation. The increases of the water resource deteriorations are due to the continuous addition of industrial effluents containing undesirable heavy metals and dyes into the water bodies (Rangabhashiyam et al., 2014a). Most of the industrial wastewater pollutants are highly persistent in nature otherwise convert into the recalcitrant form (Ayman et al., 2014). The water contamination posed various hazardous effects to the living organisms, human beings and significant damage to the environment (Xinsheng et al., 2015). Numerous conventional technologies are applied worldwide for the removal of wastewater pollutants. Nevertheless, the commercial level application with the merits of economical, effective removal at low concentration, free from secondary pollution formation and rapid treatment are still a challenging problem. In these regard, it is utmost importance to find sustainable treatment technologies for the sequestrations of heavy metals and dyes before discharge into the environment and to attain the recommended water quality requirements (Jain et al., 2016; Ehsan et al., 2017; Rangabhashiyam and Balasubramanian, 2018).

The adsorption process is the widely used superior technique because of its higher efficiency, convenient operation and feasibility in the large-scale removal process. The success outcome of the adsorption technology largely based on the use of suitable adsorbent, therefore the utilisation of cheap, non-toxic and recyclable adsorbent is the major concern of this method (Pellera et al., 2012; Rangabhashiyam and Selvaraju, 2015a). Biochar is a solid carbon-rich, fine-grained and porous material with aromatic surfaces produced by means of the thermal decomposition of biomass under the limited oxygen conditions (Xu et al., 2011). Biochar find its wide applications in soil amendment (Mukherjee et al., 2014), as carbon sequestration agent (Tarek et al., 2015), in fuel cells (Jinshuai et al., 2014) and supercapacitors (Rakesh et al., 2015). In comparison with the commercial activated carbon, biochar emerged as the new potential adsorbent. Biochar successfully subjected as the highly efficient and economical material for the adsorption of diverse pollutants. The specific adsorption properties of biochar towards pollutants removal from aqueous solutions are attributed to the distribution of porous structure, presence of higher surface area and enhanced surface chemical properties. The effective contaminant adsorption properties of biochar depend on the other factors

* Corresponding authors.
E-mail addresses: rambhashiyam@gmail.com (R. S), biobala@nitrkl.ac.in (B. P).

https://doi.org/10.1016/j.indcrop.2018.11.041
Received 22 May 2018; Received in revised form 14 November 2018; Accepted 17 November 2018

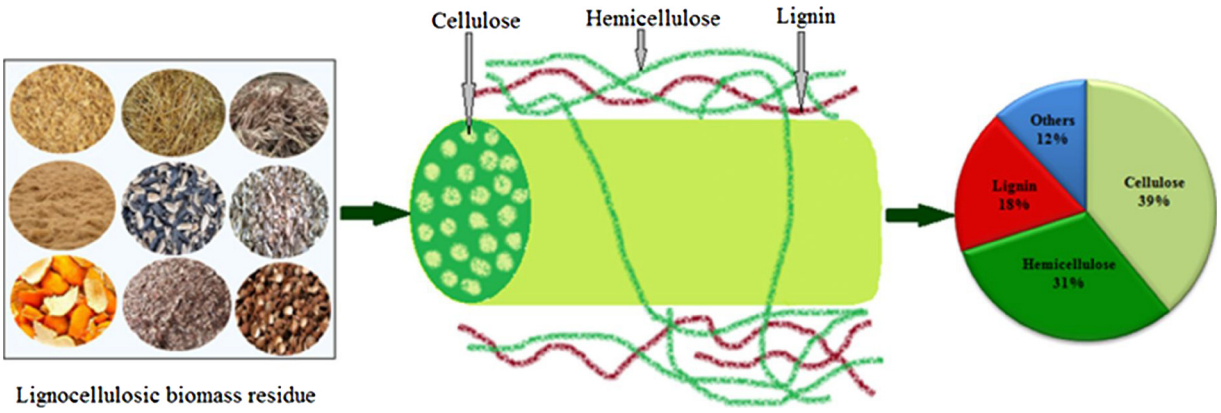

Fig. 1. The major constituents of the lignocellulosic biomass residue (Gallezot, 2012; Basu, 2010; Abdolali et al., 2014; Sonil et al., 2014; Yu et al., 2017).

like hydrophobicity, alkalinity, ion-exchange capacity and elemental compositions (Lee et al., 2015; Joyce et al., 2017; Brassard et al., 2016). In this review, the feedstock sources from various lignocellulosic biomasses for the production of biochar are discussed. The different methods for the biochar production and the modification procedures to enhance the biochar properties are reviewed. The recent research on the use of biochar for the adsorption of wastewater pollutants and associted mechanisms were reported.

2. Feedstock source of lignocellulosic biomass for biochar production

Lignocellulose utilization has gained the worldwide attention due to their property of green, copious distribution and renewable resource. The residues from agricultural activities and forest environment are the important source of the lignocellulosic biomass. The major chemical constituents of the lignocellulosic biomass include cellulose, hemicellulose, lignin and their percentage dry weight composition are approximately 39, 31 and 18 wt% (Fig. 1), respectively (Gallezot, 2012; Basu, 2010; Abdolali et al., 2014; Sonil et al., 2014; Yu et al., 2017). The chemical composition of various lignocellulosic biomass residues (Vaibhav and Thallada, 2017; Abdolali et al., 2014) are shown in Table 1. Cellulose is the major constituent of the lignocellulosic biomass consisting of β–D-glucopyranose sugar units. The linear polymer structure of cellulose is derived from the glucose dehydration. Cellulose, the main constituent of plant cell wall provides the structural support. The supramolecular structural analysis of the cellulose revealed that crystalline and non-crystalline phases intertwine with each other to form the microfibrils. Hemicelluloses are polysaccharide polymers, have lower degree of polymerization compared to cellulose. The hemicelluloses polymer are not crystalline, the variation in the structure and composition depends on the source of the lignocellulosic biomass (Andres, 2016). Lignin is a heterogeneous, complex, large molecular structure with cross-linked three-dimensional phenyl-propane polymer of phenolic monomers. Lignin is a highly branched structure, amorphous and closely associated with polymers of cellulose and hemicellulose (Rangabhashiyam et al., 2014b).

The predominant factor over the characteristic features of the biochar production is the unique nature and molecular structure of the lignocellulosic precursor used. The weight, main constituents of the lignocellulosic materials and the thermal decomposition determines over the carbonaceous structure of the biochar. The difference in reactivity of the lignocellulosic constituents tends them to undergo carbonization decomposition at the different heating rates and specific range of the pyrolysis temperature. Apart from the lignocellulosic precursor and pyrolysis temperature, the thermal transformation of cellulose, hemicellulose and lignin will also depends on the experimental conditions of the biochar production (Nan et al., 2017a, 2017b;

Table 1
The chemical composition of cellulose, hemicellulose and lignin in different lignocellulosic feedstocks (Vaibhav and Thallada, 2017; Abdolali et al., 2014).

Biomass residue	Cellulose (%)	Hemicellulose (%)	Lignin (%)
Bamboo	26–43	15–26	21–31
Barley straw	30–35	24–29	14–15
Bast fibre jute	45–53	18–21	21–26
Corncob	35–45	35–45	5–15
Coir pith	29	15	31
Cotton waste	80–95	5–20	–
Esparto grass	33–38	27–32	17–19
Flax straw	29	27	22
Groundnut shell	36	19	30
Grass	30–40	35–50	10–25
Hardwood bark	22–40	20–38	30–55
Millet husk	33	27	14
Nut shell	25–35	25–30	30–40
Oak	43	22	35
Olive stone	30–35	20–30	20–25
Oat straw	31–37	27–38	16–19
Orchard grass	32	40	5
Pine	46	24	27
Poplar wood	35	17	26
Rice straw	25–35	20–30	10–15
Rye straw	33–35	27–30	16–19
Spruce	47	22	29
Sugarcane bagasse	32–44	25–35	19–24
Switch grass	45	31	12
Subabul wood	40	24	25
Sweet sorghum bagasse	45	25	18
Wheat straw	30–35	26–32	16–21

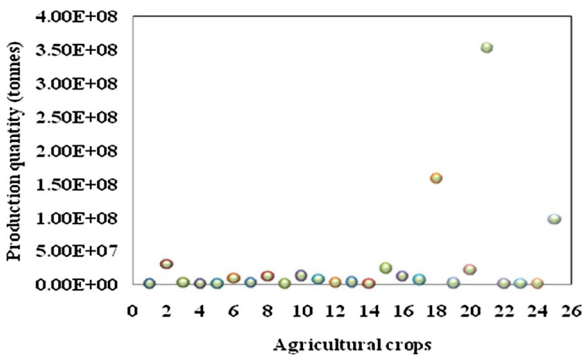

Fig. 2. The data of annual agricultural crops production in India (1. Areca nut, 2. Banana, 3. Barley, 4. Bast fibre, 5. Cashew nut, 6. Cassava, 7. Castor oil seed, 8. Coconut, 9. Coir, 10. Cotton seed, 11. Groundnut, 12. Jute, 13. Lemon, 14. Linseed, 15. Maize, 16. Millet, 17. Papaya, 18. Paddy, 19. Rubber, 20. Seed cotton, 21. Sugarcane, 22. Sunflower seed, 23. Walnut, 24. Watermelon, 25. Wheat) (FAOSTAT, 2014).

Islam et al., 2015a).

The major lignocellulosic biomass resources in India are from the agricultural sector. The FAOSTAT data 2014 on the different crop production in India was presented in Fig. 2. The large quantity of crop production generates the huge biomass of the crop residue as by-product. In India the annual production of crop residue biomass was about 686 metric tons. The sugarcane is the leading crop in terms of the production quantity and biomass residue generation followed by the rice crop. Various sources of the lignocellulosic materials were used for the production of biochar. The biomass precursors used for the biochar production includes (Khan et al., 2015), eucalyptus saw dust (Lei et al., 2015a), waste biomass of *Arundo donax* and *Phoenix canariensis* (Ricardo et al., 2017), *Astragalus membranaceus* residue (Jingge et al., 2016), crop residues (Xu et al., 2011), sugarcane pulp (Yang et al., 2013), *Astragalus mongholicus* residue (Shang et al., 2016), crop straw (Jingjian et al., 2013), Brazilian pepper wood (Yao et al., 2012), wheat straw (Yanan et al., 2016), almond shell (Klasson et al., 2013), *Hibiscus cannabinus* fiber (Mahmoud et al., 2012), orange peel (Chen and Chen, (2009)), wood chips (Reddy et al., 2014), hardwood (Chen et al., 2011a, 2011b), rice husk (Pellera et al., 2012), eucalyptus sawdust (Shungang et al., 2016), *Parthenium hysterophorus* (Sandip et al., 2017), mung bean husk (Sandip et al., 2016), *Rosa damascena* root and *Eucalyptus citriodora* stem (Puja et al., 2013), etc.

3. Production of biochar

The thermal treatment of biomass generates biochar along with other major liquids, gaseous components like bio-oil, volatile compounds, hydrogen, carbon dioxide, methane etc. The gaseous mixtures are referred to as the syngas. The biochar composed of highly stable aromatic carbon forms, which prevents the readily return of carbon dioxide to the atmosphere even in the suitable environmental conditions. Biochar produced from the resultant of the thermal treatment possess higher energy density of greater than 28 kJ/g. The thermal processes for the production of biochar product towards the application of heavy metal and dye removal are covered here (Hoda et al., 2016; Mohan et al., 2006; Lehmann, 2007). Production of biochar using the feedstock source in the form of waste and by-products has gained more attraction among the researchers, since the economic factor of feedstock determines the feasibility in large-scale production of biochar (Leng et al., 2015). The waste or residual lignocellulosic biomasses are abundant and renewable feedstock, acts as the potential and sustainable precursors for the production of biochar (Kim et al., 2011). The Lignocellulosic biomasses feedstocks are broadly divided into the categories of agricultural residues (e.g., sugarcane bagasse, straw, stalk, husk, etc.), forest residues (e.g., wood chips, branches, foliage, roots, sawdust, insect infested wood etc.), and herbaceous biomass (Miscanthus, switch grass, prairie grass, timothy grass, elephant grass, etc.) (Pu et al., 2008; Kifayat et al., 2015).

The different technologies for the conversion of biomass into biochar include pyrolysis, torrefaction, gasification and hydrothermal carbonization (Meyer et al., 2011). Biochar produced through the pyrolysis technology subjects the biomass under thermal treatment in oxygen free conditions (Islam et al., 2016). The pyrolytic conversion of biomass releases moisture, carbon dioxide, carbon monoxide, hydrogen, methane and light incondensable hydrocarbons. The liquid product mainly consists of organic (bio-oil) and aqueous phase; soluble organic species are dissolved in the aqueous phase. Leaving behind a solid residue called biochar, which is porous structure retained with the chemical functional groups and aromatic compounds (Tan et al., 2017; Caprariis et al., 2015; Xu et al., 2017).

In most of the pyrolysis process, the parametric conditions of higher heating rate, lower pressure, higher reactor temperature, smaller biomass particle sizes demonstrated increased biochar yield with high carbon content, higher surface area, better pore volume, etc. (Mohan et al., 2006; Tripathi et al., 2016; Dengyu et al., 2016a, 2016b). The process of torrefaction enables the energy densification and homogenization of biomass. The process involves the heat treatment of biomass under atmospheric pressure, temperature range of 200–300 °C, without oxygen or with limited oxygen supplies (Rousset et al., 2011). The torrefaction process produces the material with the property of less moisture, higher calorific value, lesser weight, low O/C and H/C ratio, increased hydrophobic nature, resistance to degradation from biological activity. Moreover, the torrefaction process conditions breaks the bonds present between the polymers of lignocellulosic biomass, causes the cellulose and hemicellulose depolymerization, lessen the biomass tenacity and thereby improves grindability (Antal and Gronli, 2003; Wilk et al., 2015; Pimchuai et al., 2010; Zhang et al., 2014a). The process of torrefaction yields the product with property of high energy density (Chen et al., 2012).

The process of gasification performed by the conversion of biomass into gases through gasification chamber, carried out in atmospheric pressure or under elevated pressure at higher temperature (Lee et al., 2010). The gasifying agents like air, steam, and air-steam, etc., are used for the production of syngas (Lv et al., 2004). In comparison to the biomass gasification, the gasification of biochar gasification is relatively slower. The difference are attributed to the fact that during the process of biomass gasification 80% mass loss occurs because of the loss of some permanent gases and volatile components. The carbon dioxide released during the gasification process also functions as the gasifying reagent. Even the fewer amounts of tars generated during pyrolysis step, cracks the biochar surface and deposit carbon, which consecutively reduces the gasifying reagents access and affects the effectiveness of the biochar gasification process (Di, 2008; Nzihou et al., 2013). The parameters controlling the process of gasification are temperature, pressure, gasification agent and gasification agent to the biomass ratio. Temperature is one of the significant parameter, which directly influences over the gasification process. The increase of temperature favors the production of hydrogen, carbon monoxide and carbon, whereas tar, hydrocarbons, carbon dioxide and methane content are reduced (Taba et al., 2012). The yield of the solid biochar and its carbon content using gasification process is significantly lower (Dias et al., 2017).

Hydrothermal carbonization conducted by submerging feedstock biomass into water in a sealed confined system and heated at the temperature range of 175–300 °C upto 16 h under saturated pressure. Hydrothermal carbonization also called as wet pyrolysis. The mild reaction condition of the hydrothermal carbonization process and the presence of subcritical water produce the biochar with large amount of functional groups (Liu et al., 2010). The other hydrothermal process based on the temperature range includes hydrothermal liquefaction and hydrothermal gasification. Parameter such as the residence time, process temperature, pressure and ratio of water-biomass are reported as the vital parameters in determining the property of the hyrochar (Roman et al., 2012; Sabio et al., 2016). Hydrothermal carbonization produces hydrochar without tar, which allows easy separation from the reaction solution. The process is spontaneous and exothermic in nature and thereby the various carbon from the initial products also distributed in the final product. The formation of the hydrochar occurs through a series of simultaneous reactions such as hydrolysis, dehydration, aromatization, condensation and decarboxylation. Aliphatic compounds are the major constituents in the hydrochar rather than aromatic compounds in biochars (Islam et al., 2015b; Lu et al., 2014). Hydrochar possess more oxygen functional groups and higher cation exchange capacity (Liu et al., 2010; Huff et al., 2014). Hydrothermal carbonization consumes higher energy for the hydrochar production. Even though the hydrothermal carbonizations make use of the wet biomass feedstock, the thermal energy of the process depends on the moisture content and the ratio of water-biomass (Vithanage et al., 2017). Hydrochar generally has lower surface area, readily biodegradable, poor microporosity and lower carbon stability (Hao et al., 2013). The yield of the solid biochar from the process of gasification is considerably lower compared to the other thermal technologies like

torrefaction, gasification and hydrothermal carbonization. Even though the thermal technologies commonly favored the formation of main product like bio-oil or syngas production, the byproduct left in the form of solid residue-biochar holds good removal capacity towards the removal of wastewater pollutants (Mohammad et al., 2016; Gang et al., 2017). Among the thermal technologies, pyrolysis has been reported as the most explored technique and approved as one of the best technologies for the production of biochar (Xuefei et al., 2014).

3.1. Mechanistic aspects of pyrolysis

Pyrolysis is the thermal decomposition of lignocellulose biomass by heating at the elevated temperature in the absence of oxygen supply. Pyrolysis is the first step during the combustion and gasification process. The process of the biomass pyrolysis results in the formation of carbon rich solid product - biochar, condensable and non-condensable volatiles products. The condensable volatile products are in the liquid phase, refers to bio-oil. The non-condensable volatiles are gases mainly include carbon dioxide, carbon monoxide, hydrogen, methane and C_1–C_2 hydrocarbons (Mohan et al., 2006; Pehlivan et al., 2017). The lignocellulosic biomass constituent of lignin, cellulose and hemicellulose during pyrolysis process undergoes different pathways to produce various pyrolysis products (Haiping et al., 2007). The pyrolysis investigations of each of the lignocellulosic components are essential to understand the biomass decomposition through the pyrolysis reaction pathways (Kim et al., 2016). The hemicellulose with its branched polymer structure and short side chains gets pyrolyzed easily at the temperature range of 200–350 °C. Cellulose is thermally stable due to the presence of semi crystalline array chains linked with each another; decompose in the temperature range of 305–375 °C. Lignin consists of complicated structure with phenolic polymers undergoes decomposition steadily over the temperature range of 250–500 °C (Kong et al., 2014).

The natural fibers such as cotton linter, flax, sugar cane, bamboo, hemp, and coir were analyzed for the effects of lignocellulosic components during the pyrolysis process. The natural fibers distributed with higher level of lignin content showed high yield of biochar. Biomass composed of low lignin and high cellulose content affects the thermal process and results in the incomplete fibers combustion (Dorez et al., 2014). The thermal kinetics and the activation energy values of cellulose, hemicellulose and lignin pyrolysis are related with the thermostability. The lignin pyrolysis produced high biochar yield of 61% and very low liquids yield of 0.5%; values are relatively higher than from cellulose and hemicellulose. The liquids produced from the pyrolysis of cellulose and hemicellulose includes major products like aldehydes, ketones and furans (Cui et al., 2016). The pyrolysis of the biomass produced volatile products released mainly from cellulose and hemicellulose, whereas the lignin from biomass prolysis contributes mainly to the biochar production (Thomsen et al., 2011; Shurong et al., 2017).

The lignocellulose biomass pyrolysis is a complex process due to the difference in the biomass components decomposition reaction mechanisms, thermal treatment conditions and pyrolysis reactor design. The pyrolysis of biomass takes place through a number of reactions by parallel and series, such as isomerization, aromatization, dehydration, decarboxylation, depolymerisation, and charring. The thermal heating of the biomass causes breakage of the different chemical bonds present in the polymers, releases volatile compounds and rearrangement reactions occurs within the residue matrix. These reactions represents the primary decomposition, followed with that, some of the unstable volatile compounds undergoes further conversions referred to as the secondary reactions (Vamvuka et al., 2011; Lange, 2007; Van et al., 2010; Hosoya et al., 2007).

The primary decomposition is mainly accountable for the largest biomass degradation and forms biochar at the temperature range of 200–500 °C. With the further increase of the process temperature, the secondary reactions occur within the solid matrix (Fisher et al., 2002).

Fig. 3 shows the primary and secondary mechanisms of lignocellulose decomposition by pyrolysis process. The biomass pyrolysis mechanism is greatly influenced by the major components of the lignocellulosic biomass, since they differ in the chemical structures. The cellulose precursor for the biochar formation was a polymer type of hydroxyaromatic and furanoid skeletons. During the process of pyrolysis, cellulose undergoes conversion to form amorphous cellulose intermediate, then irregular carbohydrate and aromatic carbons as the final product. The complex reactions associated with the formation of highly aromatic char includes the cellulose conversion by decarbonylation, dehydration, ring opening, aromatization, dehydrogenation and deoxygenation (Wooten et al., 2004; Xin et al., 2015). The formation of biochar occurs through the biomass conversion into a solid residue and presents an aromatic polycyclic structure. The conversion favored by the reactions of intramolecular and intermolecular rearrangements, resultant in the biochar formation with highly arranged structure and thermal stability (McGrath et al., 2003). Dehydration occurs during the process of cellulose pyrolysis was because of the hydrogen bonds cleavage, represents the primary reaction carried out at temperatures less than 300 °C. At the temperature of greater than 300 °C, dehydration occurs inter-molecularly (Xin et al., 2015). With the increase of the process temperature, the disordered agglomers of the hemicellulose char are converted into smooth and porous form, the content of functional groups like hydroxyl, methoxyl groups reduces and results in the aromaticity improvement (Lv et al., 2010; Xin et al., 2013). The higher pore size in the biochar are because of the xylan branched structure (Sharma et al., 2004). The thermal treatment of cellulose competes with reaction types of both depolymerization and fragmentation (Wang et al., 2014). The cellulose undergoes decomposition forming depolymerized cellulose through the breakdown of glycosidic bonds, finally results in the formation of short chains of glucose units. The pyrolysis process involves the different rearrangement and fragmentation products such as the furans, unsaturated hydrocarbon chains, hydroxyaromatics and fresh oxygenated groups. With the progress of the pyrolysis, the oligomeric sugars from the molten cellulose undergo different reactions like cross-linking, dehydration and fragmentation (Mamleev et al., 2009; Matthew et al., 2017). The biochar deformation in the form of melting was occurred at higher heating rates. The model of Functional group-Depolymerization, Vaporization and Cross-linking (Anna et al., 2015) explained the biochar fluidity during the lignin pyrolysis. Cellulose on fragmentation generates oligosaccharides and then monosaccharides. Cellulose gets hydrolyzed at temperatures greater than 230 °C, produces glucose monomers and hemicelluloses near 100 °C produces pentose monomers-xylose (Peterson et al., 2008). The primary mechanisms of depolymerisation and fragmentation are dominant at the higher temperature of the pyrolysis process. The presence of acids bases, salts and cations have higher impact on the pyrolysis mechanism. The cellulose selectivity in the fragmentation and depolymerisation was higher at 70–80 wt% (Manon et al., 2010). The cations act as the catalysts, induces the monomers biomass fragmentation rather than the depolymerisation, such reaction favors the formation of biochar and lowers the yield of bio-oil (Eom et al., 2012; Collard et al., 2012). The depolymerisation reaction during the primary mechanisms produces volatile organics, anhydrohexoses, levoglucosenone, levoglucosan, furans, etc (Alen et al., 1996).

The primary reactions of the biomass pyrolysis are followed by the secondary reactions of cracking and repolymerisation. Secondary reactions occur in the vapour phase or in the phase between solid and vapour, mostly to produces gases (Manon et al., 2010). The lower rate of vapor condensation consequent to the secondary reactions, which decrease the bio-oil yields because of the release of water vapor and non-condensable gases (Sonil et al., 2014). The secondary mechanism of cracking reactions involves the volatile compounds chemical bonds breakage and the formation of lower molecular weight molecules. The light hydrocarbon methane mostly responsible for the breakdown of weakly bonded groups like methoxyl, methylene and the secondary

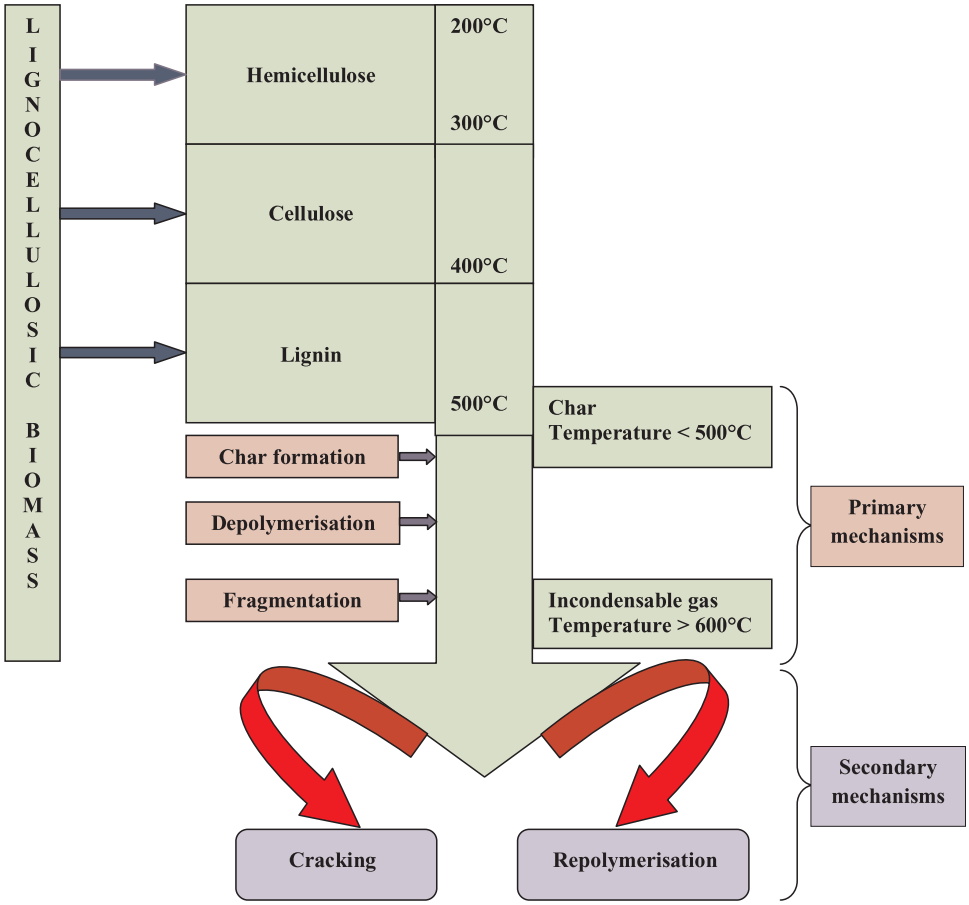

Fig. 3. Primary and secondary mechanisms of lignocellulose thermal decomposition.

decomposition of the oxygenated compounds. At high temperature hydrogen results due to the secondary decomposition, reorganization of the groups of aromatic C═C and C−H (Uddin et al., 2014; Liu et al., 2008). During the biomass pyrolysis, the monomers derived from the lignin with vinyl groups, pyran and furan compounds readily undergo the secondary reactions compared to the other products (Butler et al., 2013). The biochar from the pyrolysis of cellulose catalyze the secondary reactions for the gas formation from the volatile products, further the levoglucosan decomposition into the products like dehydrated pyranose and furans (Zhang et al., 2014a). Repolymerisation or recombination involves the volatile compounds combination to produce the higher molecular weight molecules and there are no longer volatiles in the reactor temperature conditions. The reaction of repolymerisation inside the polymer pores resultant in the secondary char formation. The distribution of polycyclic aromatic hydrocarbons in the gas phase favors the recombination reactions (Morf et al., 2002; Wei et al., 2006). The principle constituent in the biomass rather than the synergetic effects governs the primary and secondary reactions of the pyrolysis mechanism (Manon et al., 2010).

3.2. Parametric influence on lignocellulosic biomass pyrolysis

The characteristics feature of the biochar from the pyrolysis process depends on the parameters like biomass feedstock, temperature, heating rate and residence time. Most of the carbonaceous biomass can be subjected under the thermal treatment for biochar production, but the evaluation to make use of waste biomass needed based on the significant factors like eco-friendliness and cost-effectiveness (Roberts et al., 2010). In this regard, lignocellulose source of feedstock has been considered for the production of biochar through pyrolysis process.

3.2.1. Effect of lignocellulosic feedstocks

The lignocellulose biomass acts as the renewable biomass, rich in carbon compositions and recognized as the valuable precursor for the production of biochar (Xuan et al., 2014). The lignocellulose source from agricultural waste is advantageous since the agricultural crops cultivation requires less area, shorter cultivation period, non-edible and mostly considered as the waste biomass (Zanzi et al., 1996). The distribution of biopolymers in the biomass such as the cellulose, hemicellulose and lignin has great impact on the biochar production (Marion et al., 2013). The variations of the relative mass ratios of the organic and inorganic elements with the biomass are due to the different harvesting time and environmental growth conditions. The pyrolysis process of the each biomass constituents with individual thermochemical characteristics undergoes unique mechanisms for the production of biochar along with byproducts (Stefanidis et al., 2014; Yang et al., 2007). The moisture contents of biomass analysis is important, since the biomass feedstocks with more moisture and large particle sizes needs more energy for the pyrolysis process. Moreover, some carbon in the biomass undergoes burning in order to provide the required energy and therefore less biomass is converted into biochar and byproducts (Kwapinski et al., 2010). Biomass contented with more volatile matters favors highest conversion and produce bio-oil, whereas the biomass constituted with high fixed carbon shows the suitability towards the biochar production (Vaibhav and Thallada, 2017). The decomposition of lignocellulosic biomass is a complex process associated with large number of diverse reactions (Damartzis et al., 2011). The pyrolysis of biomass includes the stages of moisture evolution, followed with the decomposition of hemicellulose, cellulose, and lignin respectively. The pyrolysis of biomass is probably because of the superposition of the main lignocellulosic components (Yang et al., 2007). The biomass of wood and grass produced the different category of biochar for the

temperature increase from 100 to 700 °C. The biomass of pine needles decomposed from the amorphous form of aliphatic biochar into condensed form of aromatic biochar, with the increase of the temperature range from 100 to 300 °C to 400–700 °C (Chen et al., 2008). For the examination of the mechanism of the biomass pyrolysis process, the pure substances of cellulose, hemicellulose and lignin were employed (Stefanidis et al., 2014). Mostly the lignocellulosic feedstock biomass contented with high lignin results in the higher yield of biochar production (Sohi et al., 2010).

3.2.2. Effect of temperature

The pyrolysis process temperature plays important role in the production distribution and control on the biochar nature from the given quantity of the biomass feedstock. At the higher pyrolysis temperature, the yield of the biochar decreases with the increase of gases yield (Angin, 2013). When the process temperature is too high, biochar exhibits carbon loss with more functional group elements on its surface. The physico-chemical properties of the biochar such as pH, surface charge, elemental composition, ash content, volatile matter content, fixed carbon content, surface area, thermal stability, cation-exchange capacity, etc. are based on the pyrolysis temperature (Yuan et al., 2013; Chen et al., 2014; Shaaban et al., 2014). The increased surface area of the biochar at the higher production temperature was because of volatile substances release from biomass leaving channel structures. Such structure enhances the biochar surface area and pore structure (Kim et al., 2013; Li et al., 2013). Biochar obtained as a result of low temperature demonstrated low hydrophobicity, aromaticity, higher polarity and surface acidity. Most of the decomposition of biomass occurs between the pyrolysis temperature of 200 and 500 °C. The steps of the biomass pyrolysis are partial decomposition of hemicellulose, complete hemicellulose decomposition followed with the decomposition of whole cellulose and partial lignin decomposition (Rutherford et al., 2012). The pyrolysis at the lower temperature causes biomass to decompose into primary volatiles. The yields of biochar decline are compensated by the liquid products production at higher temperature. At the temperature of above 500 °C, the pyrolytic liquids yields decreases rapidly and compensated by increase of gas yield (Daniel et al., 2011). Temperature affects the volatilization of alkali and alkaline metals in the biomass. The bulk release occurs at greater than 500 °C and this was because of the release of the inorganic salts. The alkali metals release at less than 500 °C was mainly associated with biomass organic structure decomposition (Kowalski et al., 2007; Helena et al., 2015).

The pyrolytic temperature and nature of the lignocellulosic feedstock determines on the elemental composition of biochar. The influences of the temperature on the elemental composition of biochars produced from different lignocellulosic biomass source are represented in Table 2. The carbon content increased with the increase of pyrolysis temperature, whereas hydrogen, nitrogen and oxygen decreased. Biochars with higher content of carbon condensed aromatic rings possess only small number of functional groups. At the higher pyrolysis temperature, the atomic ratios of H/C, N/C and O/C were decreased and these are attributed to the decrease in functional groups like hydroxyl, amino and carboxylic respectively. The atomic ratio of O/C denotes of the surface hydrophilicity, provides information on the occurrence of polar functional groups on the biochar surface. The low value of the atomic ratio O/C at the higher temperature corresponds to biochar with more aromatic and lesser hydrophilic surfaces because of polar functional groups loss and more carbonization (Ahmad et al., 2012; Reguyal et al., 2017). In contrast, biochars obtained at the low pyrolysis temperature composed of amorphous carbon (Chen et al., 2017). A plot of van Krevelen was constructed with reference to atomic ratios of H/C and O/C of biochars from various lignocellulosic biomasses produced at different pyrolysis temperatures (Fig. 4). The diagram of van Krevelen acts as the indices, predicts the biochar stability as a function of pyrolysis parameters such as biomass, volatile matter content and temperature. The atomic ration H/C and O/C was lower at the higher

Table 2
Effect of pyrolysis temperature on the elemental composition of biochars produced from different lignocellulosic biomass.

Type of Biochar	Temperature (°C)	C (%)	H (%)	N (%)	O (%)	References
Pine needles	100	50.87	6.15	0.71	42.27	Chen et al., 2008
	200	57.10	5.71	0.88	36.31	
	250	61.24	5.54	0.86	32.36	
	300	68.87	4.31	1.08	25.74	
	400	77.85	2.95	1.16	18.04	
	500	81.67	2.26	1.11	14.96	
	600	85.36	1.85	0.98	11.81	
	700	86.51	1.28	1.13	11.08	
Orange peel	150	50.60	6.20	1.75	41.00	Chen and Chen, (2009)
	200	57.90	5.53	1.88	34.40	
	250	65.10	5.12	2.22	26.50	
	300	69.30	4.51	2.36	22.20	
	350	73.20	4.19	2.30	18.30	
	400	71.70	3.48	1.92	20.80	
	500	71.40	2.25	1.83	20.30	
	600	77.80	1.97	1.80	14.40	
	150	50.60	6.20	1.75	41.00	
Pine shaving	100	50.60	6.68	0.05	42.70	Keiluweit et al., 2010
	200	50.90	6.95	0.04	42.20	
	300	54.80	6.50	0.05	38.70	
	400	74.10	4.95	0.06	20.90	
	500	81.90	3.54	0.08	14.50	
	600	89.00	2.99	0.06	8.00	
	700	92.30	1.62	0.08	6.00	
Fescue straw	100	48.60	7.25	0.64	44.10	Keiluweit et al., 2010
	200	47.20	7.11	0.61	45.10	
	300	59.70	6.64	1.02	32.70	
	400	77.30	4.70	1.24	16.70	
	500	82.20	3.32	1.09	13.40	
	600	89.00	2.47	0.99	7.60	
	700	94.20	1.53	0.70	3.60	
Cotton seed hull	200	51.90	6.00	0.60	40.50	Uchimiya et al., 2011
	350	77.00	4.53	1.90	15.70	
	500	87.50	2.82	1.50	7.60	
	650	91.00	1.26	1.60	5.90	
	800	90.00	0.60	1.90	7.00	
Sawdust	400	71.50	4.70	0.05	23.60	Azargohar et al., 2013
	475	80.40	3.80	0.10	15.70	
	550	81.30	3.60	0.20	14.90	
Safflower seed cake	400	68.76	4.07	3.77	23.49	Angin, 2013
	450	70.43	3.49	3.69	22.39	
	500	71.37	2.96	3.91	21.76	
	550	72.96	2.67	3.74	20.63	
	600	73.72	2.34	3.84	20.10	
Sesame straw	300	58.10	5.20	2.40	33.40	Park et al., 2015
	400	61.70	4.70	2.50	31.20	
	500	64.20	4.20	2.70	30.20	
	600	72.60	2.10	2.90	21.70	
Rice straw	400	34.24	3.31	1.50	37.6	Guohua et al., 2016
	500	47.55	1.23	1.02	34.83	
	600	67.34	0.85	0.89	24.17	
	700	76.21	0.59	0.60	15.62	
Date palm	300	57.99	4.08	0.54	20.82	Adel et al., 2016
	700	73.42	1.14	0.35	3.19	
	700	71.60	1.76	1.72	22.20	
Sugarcane bagasse	300	44.53	5.94	0.23	35.56	Sun et al., 2017
	400	55.66	5.44	0.54	28.26	
	500	55.12	5.30	0.39	18.78	
	600	66.86	5.18	0.47	14.88	
	400	73.7	2.93	0.15	20.9	Katerina et al., 2017
	450	73.1	2.48	0.17	16.5	
	500	74.5	2.54	0.17	12.9	
	550	75.5	2.41	0.23	11.7	
	600	76.8	2.06	0.17	9.39	
Maize	400	59.8	2.80	2.08	13.7	Katerina et al., 2017
	450	58.8	2.15	1.88	14.2	
	500	54.9	2.05	1.95	13.8	
	550	44.2	1.56	1.79	16.7	
	600	29.0	1.07	1.22	23.9	

(*continued on next page*)

Table 2 (*continued*)

Type of Biochar	Temperature (°C)	C (%)	H (%)	N (%)	O (%)	References
Bark wood	400	62.5	2.65	1.12	21.8	Katerina et al., 2017
	450	63.6	2.35	1.17	20.2	
	500	63.8	2.21	1.11	19.1	
	550	62.8	1.97	1.01	19.3	
	600	68.3	1.78	0.99	13.2	
Wheat straw	400	70.6	3.50	4.46	15.8	Katerina et al., 2017
	450	69.2	3.00	4.12	17.6	
	500	71.5	2.35	4.54	14.6	
	550	70.8	2.10	4.61	13.7	
	600	73.4	1.85	4.62	11.7	
Wheat grain	400	61.1	2.84	1.30	12.0	Katerina et al., 2017
	450	62.6	2.45	1.25	9.64	
	500	61.9	2.20	1.22	10.3	
	550	61.5	1.92	1.20	9.48	
	600	57.5	1.62	1.09	8.23	

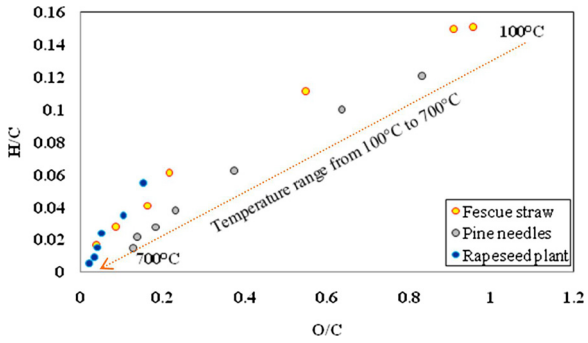

Fig. 4. The Van Krevelen plot of three lignocellulosic biomass (Fescue straw (Keiluweit et al., 2010; Pine needles (Chen et al., 2008); Rapeseed plant (Karaosmanoglu et al. (2000)) and their resulting biochars produced at peak pyrolysis temperature ranging from 100 °C to 700 °C.

biochar production temperature, the results are attributed to the demethanation, decarboxylation, decarbonylation, dehydration and depolymerization (Kim et al., 2011). The mineral content like potassium, calcium, magnesium and phosphorus increases with increasing pyrolysis temperature in the biochar (Zhang et al., 2015a). This is because the increased process temperature cause the greater extend of conversion and releases in the form of volatile products, whereas the much lesser volatile mineral compounds are retained within biochar in the concentrated form. At the higher pyrolysis temperature, the yield of biochar is lower and enriching minerals content in biochar. Besides the enrichment, at the temperature above 500 °C the minerals in biochars are more crystallized and thus become less soluble. Hence, the solubility of mineral content in the biochar diminish at the higher temperature (Zhang and Wang, 2016; Qian et al., 2016). The details on the thermal–chemical biomass conversion, the features of thermodynamic parameters are important in the design of large-scale pyrolysis reactor for the biochar production (Chen et al., 2008).

3.2.3. Effect of heating rate

The parameter of heating rate plays vital role in biomass pyrolysis since the rate of change of heat affects the characteristics features of the product upto some extent. At the lower heating rate, the likelihood of secondary pyrolysis reactions and thermal biomass cracking are reduced and consequent to the high yield of biochar. Nevertheless, pyrolysis with high heating rate enhances the yield of liquid, gaseous product and restricts the chance of biochar formation. The heating rate determines the porosity of biochar and surface area through heat and mass transfer resistance (Bouchelta et al., 2012; Boateng, 2007). The yield of biochar and volatile compounds are influenced by the heating rate of the polymers. With the low heating rates of less than 10 °C/min, the weak chemical bonds are broken and the structure of polymer are slightly affected, which allows the rearrangement reactions to form more stable matrix and inhibits the volatile compounds formation. At the very high heating rates of greater than 100 °C/s, different types of chemical bonds at the same time are broken and before the rearrangement reactions various volatile compounds are released (Neves et al., 2011).

The effect of heating rate on the yields of biochar investigated using the biomass of poplar wood. At the pyrolysis temperature of 400 °C, the increase of heating rate from 10 to 50 °C/min, showed the decrease in the yields of biochar from 34.83 to 31.95%. However, at temperature of 600 °C, there was only 0.64 wt% change. Jute dust investigated for the biochar production with the heating rates of 10 and 40 °C/min. The yield of biochar at the minimum process temperature of 400 °C decreased from 40.48% to 35.33% as the heating rates increased from 10 °C/min to 40 °C/min. These results revealed that low heating rate had great influence on the yields of biochar (Dengyu et al., 2016a, 2016b; Nabajit et al., 2014). The elemental constituents of biochar are influenced by heating rate at a particular temperature. Biochar produced from pinewood biomass at low heating rate of 2 °C/min presented higher alkaline elements concentration in comparison to biochar produced using the higher heating rate of 450 °C/min (Mohanty et al., 2013)

3.2.4. Effect of residence time

The slow or conventional pyrolysis process performed with a residence time duration from few minutes to days at moderate temperatures, slower heating rates mostly favored the production of biochar (Chen et al., 2003). The longer residence time of vapor in the pyrolysis reactor along with intermediate temperature and lower condensation rate, the secondary reactions also leads to the generation of high molecular weight compound like biochar (Bridgwater et al., 1999). The low pyrolysis temperatures and long residence time favors the biochar formation. The information of the kinetic and thermal data are important for the pyrolysis reactor design, moreover finding the residence time and the heat supply to the reactor are essential (Manon et al., 2010). The increase of the vapor residence time provides sufficient time for the constituents of biomass to undergo repolymerization reaction. Where the lesser residence time results in the incomplete repolymerization of the biomass constituents and consequent to the decreased biochar yield (Park et al., 2008). More research are performed on the influence of vapour residence time on product distribution, However the investigation of the interaction between pyrolysis temperature and vapour residence time on the product quality are limited (Tao et al., 2016). The residence time has great impact on the finishing point of carbonization process, biochar features of specific surface area and pores volumes. The longer prolonged residence time may affect the biochar surface area due to the structural melting, elemental realignment and shrinkage (Saba et al., 2017). The residence time determines over the composition of pyrolysis product, the yield of biochar reduced with the conditions of increased residence time and uniform pyrolysis temperature. The residence time controls over the surface area, micro- and macro-pores distributions on biochar. The increased residence time up to 2 h with the pyrolysis temperature of 500–900 °C showed enhanced surface area and pore area, whereas had negative effect when the residence time go beyond 2 h (Zhang et al., 2015b; Lu et al., 1995). The effect of residence time on the pyrolysis process is always determined only along with the parameters like feedstock biomass, temperature, heating rate and other parameters (Fassinou et al., 2009).

4. Aspects of biochar modification

Biochars produced from the lignocellulosic source of biomass through pyrolysis under oxygen-limited condition holds the physical and chemical surface characteristics, which find its usage in the removal of wastewater contaminants (Vithanage et al., 2015a).

Nevertheless, the applicability of biochar towards the sequestration of different contaminants are limited due to their lesser efficient. The unmodified biochars demonstrated with lower capacity of contaminants removal than some modified biochars, especially at the higher pollutants concentrations. Recently, more research has been focused on the biochar modifications through new structures, surface properties enhancement and activation methods in order to increase the adsorption efficacy towards the removal of wastewater contaminants (Zhou et al., 2014; Chen et al., 2011a; Ok et al., 2015). The biochar modifications involving various physical activation and chemical activation methods are widely discussed in the following sections.

4.1. Physical activation

The physical activations of the biochar improve the properties of specific surface area, pore volume and pore structures of the biochar. Moreover, the physical activations influences on the surface chemical properties such as the functional groups, hydrophobicity and polarity (Jung et al., 2014; Michal et al., 2017; Vithanage et al., 2013). The methods of the physical activations are mostly uncomplicated, inexpensive and do not subject chemicals. The steps in the physical activation include biomass carbonization followed with the step of activation using the agents of steam, carbon dioxide, oxygen, nitrogen, ammonia etc. (Azargohar et al., 2008; Jing et al., 2017).

4.1.1. Steam activation

Steam activation is one of the physical activation process employed for biochar modification after the synthesis. Steam activation widely applied to increase specific surface area, improves porous structure and surface properties modifications of the biochar. In this process of biochar modification the oxidizing agent of steam is employed, which is comparatively simple and cost-effective (Lou et al., 2016; Rajapaksha et al., 2016). The steam activation of the biochar involves the following reactions: exchange of oxygen from water molecule to the carbon surface and forms surface oxide and hydrogen. The hydrogen reacts with the carbon surface and forms the complexes of surface hydrogen. Further, the steam oxidizes the surface sites of the carbon and releases hydrogen and carbon dioxide, which are involved in the activation of biochar surface and also hinders the gasification reaction on the sites of carbon because of water-gas shift reactions (Bach, 2007).

The process of steam activation incorporates the functional groups containing oxygen such as ether, carbonyl, carboxylic and phenolic hydroxyl groups onto the surfaces of biochar. The cleavage of C═C bonds in the biochar during steam activation are comparable to that of the polymerization reactions which forms C═C bonds in the biochar. The extent of self-polymerization was significantly increased. The steam activation enhances the biochar hydrophilicity in spite steam is a weaker oxidant. The activation process brings out the biochar modification by the elimination of trapped products during the thermal treatment of the biomass and further oxidizes the surface of carbon by producing mainly hydrogen, carbon monoxide and carbon dioxide (Ippolito et al., 2012; Dongdong et al., 2017). The effects of the steam activation process on the biochar includes the volatile compounds elimination, new micropores formations and further widening of existing pores (Zhang et al., 2014b). Biochar produced from rice husk subjected for steam activation. The process conditions include steam flow rate of 5 mL/min for about 45 min at the maximum temperature followed from 3 h complete of pyrolysis biomass treatment (Mayakaduwa et al., 2016). The mung bean husk derived biochar was steam activated by heating the biochar up to the temperature of 650 °C at 55 °C per 15 min. The superheated steam was passed into the hot atmosphere for 1 h. Then the steam activated biochar was cooled, grinded and sieved to the desired particle size. The steam-activated biochar has highly heterogeneous porous structure and higher surface area. Increase in the carbon content from 36.94% to 59.35% reported in the steam activated biochar (Sandip et al., 2016). The parameters of the steam activation process such as the activation temperature, water vapour flow and activation time influences on the activated biochar surface area and porosity (Zhang et al., 2014b).

4.1.2. Gas activation

The activation of biochar performed using the gases such as carbon dioxide, oxygen, nitrogen, ammonia or their mixtures. The biochar activated by gas exhibits increased specific surface area and pore volume (Burhenne and Aicher, 2014). The nitrogen and oxygen activated biochar samples were produced through the thermal treatment of pine chips. The yields of nitrogen and oxygen activated biochar were 42.3% and 64.2%, respectively. The carbon contents in the oxygen activated biochar (83.8%) is higher than in the nitrogen activated biochar (72.6%). The data of the H/C ratio of oxygen activated biochar was greater than nitrogen activated biochar, represented that oxygen activated biochar was more carbonized than nitrogen activated biochar (Chanil et al., 2013). The influence of carbon dioxide on the biochar prepared from hickory and peanut hull was examined as the function of activation temperature and activation time. The surface area and pore volume of the carbon dioxide activated biochar were increased with the increase of activation temperature and activation time. Moreover, the mixtures of carbon dioxide along with other gases also enhance the surface characteristics and porous structure of the biochar (Fang et al., 2016). The gas activation depends on the biochar, gas activating agent and biochar activation conditions. The activated biochar resulted from the coffee endocarp pyrolysis using carbon dioxide presented higher specific surface area and pore size (Nabais et al., 2008). The agricultural waste biomass of cotton stalks are developed with suitable micropore structure by means of carbonization and activation using carbondi oxide. The basic nitrogen functionalities are introduced into carbon matrix of biochar through ammonia purging. At the higher temperature radicals like NH_2, NH, and H are produced from ammonia breakdown, the radicals reacts with the active sites distributed at the edges of the graphene layers in the biochar introduces N-containing functional groups (Zhang et al., 2013a; Vinke et al., 1994).

4.2. Chemical activation

The biochar chemical modification involves the simultaneous carbonization and chemical activation or carbonization of biomass and then mixed with the chemical agent for activation. The process of chemical activation is economical, generally carried out at lower temperature and in shorter time duration (Qian et al., 2015; Yorgun et al., 2009). The chemical activation demonstrates higher efficiency in the development of biochar microporosity, mineral matter reduction, activates carbonaceous materials and increases the surface functional groups, which offers the cation and anion exchange properties (Takaya et al., 2016; Lillo et al., 2003).

4.2.1. Acid and alkali treatment

The modification of biochar through acid and alkali are performed using the activating agents from inorganic acids (hydrochloric acid, sulfuric acid, nitric acid, phosphoric acid), alkali hydroxides (potassium hydroxide, sodium hydroxide) and inorganic salts respectively (zinc chloride, potassium carbonate) (Zhang et al., 2005; Ko et al., 2011; Rangabhashiyam and Selvaraju, 2015b; Unai et al., 2016). Generally, the acid activation of biochar performed by transferring biochar into the acid solutions up to the ration of 1:10 and at the temperature range from room to 120 °C. The reaction times are usually varied from hours to days (Jin et al., 2014; Ros et al., 2006). The biomass of eucalyptus sawdust impregnated with 85% phosphoric acid and carbonization performed at the fixed pyrolysis temperatures under nitrogen supply. After the activation of the biochar with phosphoric acid, the specific surface area and total pore volume was increased by 26.9 and 23.6 times. The higher atomic ratios of O/C and (N + O)/C denoted higher hydrophilicity and polarity. The FT-IR spectrum of activated biochar

showed new bands at 1160 and 1076 cm^{-1} assigned to esters, ethers, or phenol groups (Shungang et al., 2016). The hydrochloric acid treatment of biochar from kenaf fibre biomass resulted in the increase of surface area from 289.497 to 346.57 m^2/g. Moreover, the structure of the activated biochar is highly porous and showed honeycomb with various sizes (Mahmoud et al., 2012). The dehydrated fibre biomass of *Opuntia ficus indica* cactus was thermally treated to obtain the carbonized product. The produced biochar was suspended in the chemical activating agent of nitric acid for 24 h at room temperature, followed with reflux for 3 h at 80 °C under continuous stirring. The FT-IR analysis revealed that nitric acid activated biochar introduced carboxylic moieties on the biochar surface (Loukia et al., 2014). The increase of the sulfuric acid concentration for the activation from 5 to 30% had positive effect towards the increase of surface area. However, the negative effect of decreased surface areas observed at the excessive concentration of sulfuric acid (Guo et al., 2005). The sulfuric acid treatment of cotton wastes showed the higher transformations of the biochar's solid phase (Jersson and Sergio, 2015). The oxidation of biochar using sulfuric acid treatment introduces more acidic functional groups on the biochar surface. The higher percentage of oxygen consequent to the increased in the atomic rations of O/C and H/C, which inturn indicates the decrease of hydrophobicity (Vithanage et al., 2015b).

Biochar produced through the pyrolysis of poplar biomass treated with the activating agent sodium hydroxide. The determination of the Iodine number measurements indicate that the increase of biochar surface area was with respect to raise of the pyrolysis temperature and with the activation process (Caprariis et al., 2017). Potassium hydroxide used for the activation of biochar produced from whitewood. The higher surface area of 1500 m^2/g was obtained, which is comparable to that of the surface area of commercial activated carbons (Azargohar and Dalai, 2008). The horse chestnut shell powder biochar activated was immersed into aqueous solution of potassium carbonate in the ratio of 1:1. The impregnated biomass subjected for the carbonization at 700 °C with nitrogen flow. The activated biochar surface areas are in the range of 500–1500 cm^2/g (George et al., 2016). The sodium hydroxide treatment resulted in the depolymerization reaction (Jersson and Sergio, 2015). The Alkaline modification of biochar produces biochar with the larger surface area with a higher ratio of H/C, N/C and lower value of the atomic ratio of O/C. The lower ration of O/C specifies the hydrophilic nature of acid modified biochar, which decrease with the increase of biochar aromaticity. The increase of N/C ratio introduces more nitrogen containing functional groups and leads to the occurrence of basic properties on the surface of modified biochar (Ma et al., 2014). Zinc chloride, one of the activation agent used for the modification of the biochar produced from sesame straw (Park et al., 2015).

4.2.2. Impregnation methods

The minerals of different types are found suitable for the impregnation with biochar. The minerals such as hematite, magnetite, zero valent iron, amorphous hydrous manganese oxide, calcium oxide, nitrate and birnessite are used in the biochar modifications. The impregnation methods of biochar are carried out by means of soaking biochar followed by the pyrolysis, otherwise first the biochar pyrolysis and then impregnation (Wang et al., 2015c; Liu et al., 2017; Agrafioti et al., 2014). The treatment with the functional additives of calcium chloride, aluminium chloride, magnesium chloride and iron(II,III) oxide improved the surface properties of biochar (Kangning et al., 2017). Iron impregnation in biochars occurs in the different forms of iron oxide such as Fe_2O_3, Fe_3O_4, FeOOH, based on the pyrolysis conditions. Iron with the oxidation states of both ferrous and ferric are the important element in different feedstocks (Li et al., 2012). The biochars modification done by wet impregnation using iron oxides. Magnetization decreased the point of zero charge of the biochar, this was likely caused due to the surface coverage with maghemite or magnetite (Zhantao et al., 2015). The biochar impregnated with salt of ferric ion is treated at higher temperature. The biochar are prepared with maghemite used as the magnetic medium (Zhu et al., 2014). The magnetization of biochar performed by introducing it into the magnetic medium of iron or cobalt compound, which allows the biochar for the suction out in the presence of the external magnetic field towards the separation of activated biochar from the aqueous solution (Reddy and Lee, 2014). The magnetic biochars are synthesized through co-precipitation of Fe^{3+}/Fe^{2+} onto the biomass of orange peel powder, and then examined under the different pyrolysis temperature. The prepared magnetic biochar exhibited smaller surface area and larger average pore diameter compared to the non-magnetic biochar (Chen et al., 2011a).

The porous MgO-biochar nanocomposites were prepared with polycrystalline magnesium oxide and using different lignocellulose biomass. The nitrogen supply during the pyrolysis process removes byproduct hydrochloric acid and assists the formation of magnesium oxide nano particles in the matrix of biochar (Zhang et al., 2012a). The pristine biochar was impregnated using the binary oxide of Fe-Mn and Fe/Mn. Instrumental analysis of scanning electron microscope and energy dispersive spectrometer reported the presence of many pores on the Fe/Mn modified biochar (Lina et al., 2017). The tomato tissues supplemented with Mg/Ca offers the direct way to preparation of the magnesium enriched biochar, which composed of the of magnesium oxide and magnesium hydroxide nanoparticles within the biochar (Yao et al., 2013). The synthesized calcium and magnesium impregnated biochar was loaded with many calcium oxide and magnesium oxide nanoparticles and higher in organic functional groups. The increase of the synthesis temperature showed the decrease in yield, increase of carbon content, increase of surface area, decrease of hydrogen content and the nitrogen content not affected (Ci et al., 2015).

4.2.3. Microwave assisted activation

Microwave assisted pyrolysis mainly associated with the characteristics of microwave dielectric heating. The rate of heating are in the range from 0.1 °C/s to greater than 1000 °C/s. The heating rate plays vital role and strongly influences on the yield of the pyrolysis product. The lower temperature, higher homogeneous and selective heating conditions produces biochar with higher quality. Biochar produced using the microwave assisted pyrolysis are reported with higher surface area and larger pore volume (Motasemi and Afzal, 2013; Bridgwater, 2012; Luque et al., 2012). Microwave assisted heating has the advantages of internal, volumetric heating, accelerates the chemical reactions rate and reduces the energy consumption. During the microwave pyrolysis, the spots of minute microplasma are formed all through the reaction medium. This increases the local temperature, generates gases and which inturn enhances the pores formation in the biochar (Suriapparao and Vinu, 2015; Ahmed, 2016). The microwave pyrolysis of switchgrass carried out in a quartz tube reactor with microwave frequency 2.45 GHz and maximum power output 1.2 kW. The additives like potassium phosphate, clinoptilolite and bentonite were analyzed for their role in the improvement of the biochar properties. The higher clinoptilolite percentage increased the rate of heating of the biomass and thereby the microwave heating time to attain the pyrolysis temperature was reduced. This decreased the yield of biochar, because of faster pyrolysis. The potassium phosphate additive required more time to reach the pyrolysis temperature (Mohamed et al., 2016a). Therefore, the yield of biochar better increased due to the inhibition of hemicellulose devolatilization (Lu et al., 2013). The synergistic effects were the mixture of any two additives indicated increased microwave absorption rate and quality of biochar. Microwave assisted pyrolysis was conducted using the corn stover biomass for the biochar production under atmospheric pressure, with varying pyrolysis temperatures and residence time. The activated biochar showed the amount range of surface carbonyl groups from 0.27 to 1.70 mmol/g carbon, which was considerably influenced by the process parameters temperature and residence time. The surface area of the microwave assisted biochar was 45 m^2/g. The result indicates that the surface functional groups of

biochar were significantly influenced by the pyrolysis temperature and residence time (Lei et al., 2015b). The magnetic biochar using the biomass of sugarcane bagasse conducted by microwave assisted pyrolysis with the microwave power of 600 W. High magnetic biochar yield of 69% attained by microwave heating for 30 min radiation time and with ferric oxide to biomass impregnation ratio of 0.45 respectively (Noraini et al., 2016).

5. Application of biochar for the removal of wastewater contaminants

Biochar derived from the pyrolysis treatment of different source of lignocellulosic biomass are urged as a multifunctional adsorbent towards the removal of wastewater pollutants. Biochar with the superior property of surface area, cation/anion exchange capacity, porous structure and elemental composition arise the distinction in the adsorption behavior from biosorbent (Linson et al., 2016; Wang et al., 2015b). Relatively, carbon material type of adsorbents such as activated carbon and biochar are extensively developed for the removal of wastewater contaminants. In comparison with activated carbon, the preparation of biochar is simple and economical (Shan et al., 2016). In the last ten years, the number of publications pertinent to the adsorption of wastewater contaminants using biochar has been increased significantly.

5.1. Removal of heavy metals

Heavy metals from the different industrial effluents have hazardous effects of toxicity or carcinogenic and are more pronounced at higher trophic levels. Among the various heavy metal lead, cadmium, hexavalent chromium and mercury are in the top toxicity list. The property of non-biodegradability tends heavy metal for accumulation and their amounts are increased along the food chain (Volesky, 1994; Rangabhashiyam and Balasubramanian, 2016). Recently many researchers reported on the usage of biochar as adsorbent towards the metal removal.

The adsorption characteristics of biochars derived from the peat moss under different carbonization conditions were investigated for the removal of lead, copper and cadmium. The biochar produced at the pyrolysis temperature of 800 °C consists of well developed porous structures. However, at the pyrolysis temperature of 1000 °C pore structures of the biochar were damaged and contracted. The adsorption capacity of the raw biomass of peat moss towards the metals removal were lower compared to the biochar, which are due to the highly developed porous structure and higher pH of the biochar (Lee et al., 2015). The leaf of Leersia hexandra Swartz used for the biochar preparation and used for the adsorption of hexavalent chromium. The solution pH is an important factor affects the adsorption of hexavalent chromium onto the biochar. The pH parameter influences over the biochar surface charge, functional groups dissociation, ionization and speciation of hexavalent chromium. The presence of the functional groups such as OH, C−H, $-CH_2$, C═C, and C−O in the biochar are mainly involved in the adsorption of hexavalent chromium. The equilibrium adsorption data fitted with the Freundlich isotherm model. The pseudo-second-order kinetic model better described the experimental data (Xingfeng et al., 2017). Pyrolysis temperature on the production of biochar using pistachio shell positively influences on the uptake capacity for the removal of lead and copper from aqueous solutions. The equilibrium data better fit with Freundlich isotherm model makes clear that biochar produced at higher pyrolysis temperature was used. The biochars produced at the pyrolysis temperature of 550 °C showed maximum adsorption capacity towards lead and copper. The property of the biochar includes higher carbon content, porosity and distribution of pores (Kostas et al., 2015). The biochar with the characteristics of surface area and porous structure influenced the metal adsorption process. Biochar possess different magnitudes of surface area and pores distribution within the adsorbent particles, such forms offers for the metal accessibility (Khare et al., 2017). Biochars from the crop straws of canola, rice, soybean and peanut are evaluated for the adsorption of trivalent chromium. The adsorption capacity are reported in the increasing order of peanut > soybean > canola > rice, the results of the adsorption capacity are consistent with the oxygen containing functional groups in the biochar. The complexation of trivalent chromium with functional groups has major contribution in the adsorption process. The peak shifts of functional groups in the trivalent chromium loaded biochar are due to stretching of aromatic C═C ring, phenolic OH region and stretching of aliphatic C−H group (Jingjian et al., 2013).

The biochar from the two different woody biomass were used for the adsorption of cadmium, zinc and copper. The differences in surface area and cation-exchange capacity of the biochars are found using physicochemical characterization. The adsorption process are affected by both contact time and solution pH. The cadmium and zinc were bound to the biochar as the exchangeable fractions and copper as oxidizable fractions (Vladimir et al., 2015). The affinity of heavy metal is in the order of lead > chromium > copper on the binding of orchard pruning derived biochar. In case of the binary adsorption system, the presence of lead affected the adsorption of chromium and copper. The residence time of the metal on biochar surface influences the competitive adsorption. Considerable copper adsorption occurred even in the presence of higher concentration of lead and chromium, represent that biochar possess unique adsorption site for single metal (Antonio et al., 2014). The native and anaerobically digested sugarcane bagasse biochar tested for the adsorption of lead. The produced biochars showed lower surface areas. The adsorption capacity reported using the modified biochar was better. The adsorbents analysis using the negative zeta potentials specified the surfaces of the adsorbents are strong negatively charged (Inyang et al., 2011). Adsorption of copper and zinc using the biochar from softwood and hardwood favored at higher pH. The negative charge of the biochars makes the metal ions to undergo hydrolysis and polymerization. The salinity influences on the surface charge of the biochar brings out the competitive effect between the sodium, exchangeable calcium and heavy metal ions (Shasha et al., 2016). Alamo switch grass biochar produced by the thermal treatment at 300 °C. The biochar produced was activated using potassium hydroxide in order to improve the porosity and to eliminate the partially blocked pores in the biochar. Maximum removal of copper and cadmium ions attained at the solution pH 5.0. The modified biochar presented higher affinity towards the cadmium removal, while unmodified biochar showed greater affinity for the removal of copper (Regmi et al., 2012). The presence of minerals in the biochar plays vital role in the adsorption of heavy metals. The adsorption efficiency declined under the condition of demineralized biochar. Biochar modified with manganese oxide and birnessite were used to improve the adsorption capacity towards the removal of arsenic, lead and copper. Only the specific minerals in the biochar exhibits positive role for the adsorption of heavy metals (Song et al., 2014). The biochar applications for the adsorption of heavy metals are summarized in Table 3.

Different mechanisms are proposed on the adsorption of heavy metals by biochar from aqueous solutions. The possible mechanisms include surface complexation, electrostatic interactions, ion-exchange, physical adsorption, surface precipitation, co-precipitation and inner-sphere complexation (Aleksandra et al., 2015; Hongbo et al., 2017; Zhengtao et al., 2017). The adsorption mechanisms of each metal are different from one another and biochar property has major contribution in the removal mechanism. The biochar obtained from corn straw used for the adsorption of cadmium and lead from water. The adsorption removal efficiencies of 99.24% and 98.62% were attained for cadmium and lead respectively. The optimal pH range value was reported as of 4.0–7.0. The analysis of Fourier transform infrared spectroscopy and Raman analysis reveals that the adsorption of both the metals occur through the surface complexation with active adsorption sites, coordination with π electrons and precipitation with inorganic anions

Table 3
Adsorption characteristics of heavy metals removal using different biochars.

Biochar type	Pyrolysis temperature	Residence time	Heavy metal	Isotherm model	Kinetic model	Adsorption capacity (mg/g)	References
Pinewood	700 °C	2 h	Cu(II)	Langmuir	–	2.75	Liu et al., 2010
Hardwood	450 °C	< 5 s	Cu(II)	Langmuir	PSO[a]	6.79	Chen et al., 2011a
Hardwood	450 °C	< 5 s	Zn(II)	Langmuir	PSO[a]	4.54	
Corn straw	600 °C	2 h	Cu(II)	Langmuir	PSO[a]	12.52	
Corn straw	600 °C	2 h	Zn(II)	Langmuir	PSO[a]	11.0	
Peanut hull	300 °C	5 h	Pb(II)	Langmuir	Elovich	22.82	Xue et al., 2012
Rice husks	300 °C	30 min	Cu(II)	Freundlich	PSO[a]	4.570	Pellera et al., 2012
Olive pomace	300 °C	30 min	Cu(II)	Freundlich	PSO[a]	5.118	
Orange waste	300 °C	30 min	Cu(II)	Freundlich	PSO[a]	4.921	
Alamo switchgrass	300 °C	30 min	Cd(II)	–	–	34	Regmi et al., 2012
Cotton Wood	600 °C	1 h	As(V)	Langmuir	PSO[a]	3.147	Zhang et al., 2013b
Spartina alterniflora	400 °C	2 h	Cu(II)	Langmuir	PSO[a]	48.49	Li et al., 2013
Sugarcane pulp residue	500 °C	3 h	Cr(III)	Langmuir	PSO[a]	15.85	Yang et al., 2013
Rice husks	950 °C	30 min	As(V)	Langmuir	–	1.46	Cope et al., 2014
Cactus fibres	600 °C	1 h	Cu(II)	Langmuir	–	224	Loukia et al., 2014
Kans grass	500 °C	4 h	As(V)	Langmuir	PSO[a]	3.132	Baig et al., 2014
Rice hull	400 °C	5 h	Pb(II)	Langmuir	PSO[a]	367.65	Yan et al., 2014
Peat moss	800 °C	90 min	Pb(II)	Langmuir	PSO[a]	81.3	Lee et al., 2015
Peat moss	800 °C	90 min	Cu(II)	Langmuir	PSO[a]	39.8	
Peat moss	800 °C	90 min	Cd(II)	Langmuir	PSO[a]	18.2	
Pistachio shell	550 °C	60 min	Pb(II)	Freundlich	PSO[a]	1.22	Kostas et al., 2015
Pistachio shell	550 °C	60 min	Cu(II)	Freundlich	PSO[a]	1.17	
Peeled pine wood	700 °C	3 h	Pb(II)	Langmuir	PSO[a]	91.98	Wang et al., 2015a
Hickory chips	600 °C	2 h	Zn(II)	Langmuir	–	0.71	Zhuhong et al., 2016a
Chestnut shell	450 °C	2 h	As(V)	–	–	17.50	Zhou et al., 2017
Phyllostachys pubescens	450 °C	3 h	Pb(II)	Freundlich	Elovich	67.4	Chao et al., 2017
Phyllostachys pubescens	450 °C	3 h	Cd(II)	Freundlich	Elovich	14.7	
Pine chips	300 °C	15 min	Cd(II)	Langmuir-Freundlich	PSO[a]	167.3	Chang et al., 2017
Corn straw	300 °C	2 h	Cr(VI)	Langmuir	–	116.28	Nan et al., 2017a

[a] Pseudo-second-order.

(Tong et al., 2017). The biomass of peanut, canola, and soybean straw were carbonized at 400 °C with the heating rate of 20 °C/min and 3.75 h residence time, the prepared biochars were used for the adsorption of copper. The biochars reported with higher adsorption capacities at the pH range of 3.5–5.0. The higher phosphate presence in the biochars caused the formation of copper-phosphate and precipitation. The removals of copper by the biochars are associated with both adsorption and surface precipitation (Tong et al., 2011). The distribution of soluble and insoluble mineral contents in biochar plays vital role in the heavy metal removal process. The adsorption affinity of water-soluble minerals towards heavy metal ions removal is much higher than the water insoluble minerals (Xu and Chen, 2014). The biochar produced at the lower temperature have the minerals as amorphous, highly soluble and gets released readily for the successive precipitation with metal ions. Whereas the higher temperature produced biochar possess the minerals, which are more crystallized, less soluble and does not undergo easy release (Zheng et al., 2013; Cao and Harris, 2010). The increased degree of carbonization and biochar loading, the immobilization of heavy metal through cation exchange progressively more prevailed by the coordination by carbon π electrons and precipitation. The minerals solubility in the biochar controls over the exchange of the cations. The lower degree of carbonization and lower pyrolysis temperature enhance the heavy metals immobilization on the biochar, because of the higher release of mineral components like potassium and calcium (Uchimiya et al., 2010, 2012). The enhancement of the functional groups on the biochar offers more binding sites for the heavy metals. The presence of functional groups favors the biochar and metal ions interactions for the formation of surface complexes, cation-π bonding, ion-exchange and electrostatic interactions (Song et al., 2014; Wang et al., 2015b). The biochar of sugar beet tailing used for the removal of hexavalent chromium occurs through electrostatic attraction coupled reduction. At the low pH, the negatively charged hexavalent chromium species migrated on the positively charged biochar surfaces by means of the electrostatic driving forces. The migrated hexavalent chromium is reduced to trivalent chromium due to hydrogen ions participation and biochar electron donors. The reduced trivalent chromium is released to the aqueous solution and some of them are complexed with the biochar function groups (Xiaoling et al., 2011).

Biochar from the peanut hull modified using the hydrogen peroxide subjected for the adsorption of lead from the aqueous solutions. The adsorption capacity of activated biochar was 20 times more than the unmodified biochar. The results are mainly due to the more number of the carboxyl functional groups on the surface of the activated biochar (Xue et al., 2012). The effect of pH effect on the adsorption of zinc was studied using two different wood based biochars. At the solution pH range of 3.0 to 8.5, the zinc occurs as Zn(II) ions. The increase of soluble hydroxide like $Zn(OH)_2$ and $ZnOH^+$ are generated at the solution pH of above 7.5. The adsorption mechanism of precipitation and ion exchange are mainly involved into adsorption of zinc ions (Fristak et al., 2015). The bismuth oxide impregnated wheat straw biochar used for the removal of arsenic and chromium. The removal mechanisms of arsenic are associated with the exchange of ligand between bismuth atom and arsenite. The chromium removal involves the steps of the hexavalent chromium being adsorbed on the protonated biochar by electrostatic force of attraction, further reduced to trivalent chromium and fixed in the biochar. The biochar of pine wood feedstock was pyrolyzed in the presence of manganese(II) chloride tetrahydrate and the other performed by means of birnessite impregnation through precipitation. The birnessite modified biochar posses the higher oxidation potential, which involves in the better transformation of arsenite to arsenate (Zhu et al., 2016; Wang et al., 2015b). The biochar from fruit tree pruning wastes were used for lead adsorption. The morphology of the biochars was influenced by temperature of the pyrolysis process. The surface area increased with the pyrolysis temperature increase and this was attributed to the destruction of functional groups like the aliphatic alkyl, ester and aromatic lignin core exposure. The adsorption of lead by biochar includes the interactions between d-electrons of lead and aromatic π-electrons of biochars (Jong et al.,

2015). The adsorption capacity of biochar from Triticum aestivum straw was higher towards the cadmium removal, the adsorption process strongly influenced by solution pH. The equilibrium data of the cadmium and cobalt in binary system best described by the extended Langmuir isotherm model, elucidated that biochar had higher affinity towards the cadmium than cobalt. The adsorption mechanisms are due to the biochar functional groups, metal ions precipitation and the presence of minerals such as apatite, calcite and sylvite in the biochar offers the extra adsorption sites for the metals (Martin et al., 2017). More surface availability of the potassium hydroxide activated biochar for complexation and cation exchange resulted in the higher adsorption capacities by the 700 °C biochar towards the cadmium and lead ions removal. The mechanisms of ion exchange and surface complexation dominated the metal adsorption process (Yakkala et al., 2013). Biochar with the larger surface area and surface functional groups acts as an efficient reductant of hexavalent chromium to trivalent chromium. The functional groups of carboxylic and hydroxyl on the biochar surfaces possibly caused the reduction of hexavalent chromium. The irregular polycyclic aromatic hydrocarbons sheets contribute the π-electrons for the reduction of hexavalent chromium. The trivalent chromium ions are reabsorbed through the process of surface complexation and precipitation (Hsu et al., 2009; Wang et al., 2010). The heavy metal ions undergo strong ionic interactions with the anionic functional group and electron dense double bonds in the biochar. The mechanism of ion exchange makes the different functional groups as intrinsic within the structure of biochar (Trakal et al., 2016).

5.2. Removal of dyes

Dye or color is the first pollutant to be known in the industrial effluent. The effluents generate significant amount of colored wastewater and their discharge into the water bodies imposes hazardous effects to the biological systems. The toxicity effects of dyes are carcinogenic, mutagenic and allergenic. Even the presence of too little amounts of dyes of less than 1 mg/dm in water is highly visible and undesirable. Dyes are recalcitrant in nature composed of organic and inorganic constituents, resistant to degradation, stable to heat, light and oxidizing agents (Rangabhashiyam et al., 2013; Akar et al., 2009; Rangabhashiyam and Balasubramanian, 2017).

The biochar prepared from the weeds activated with nitric acid used for the adsorption of methylene blue from aqueous solution. The biochar showed lower surface area, more oxygen containing functional groups and lower point of zero charge. The maximum removal of dye was reported under the 7.4 solution pH and 50 °C (Fuat et al., 2017). The biochar produced using the eucalyptus sawdust subjected for the activation using acetic acids, citric acids and tartaric acids. The activated biochars were assessed towards the adsorption of methylene blue from aqueous solution. The citric acid activated biochar showed the largest adsorption capacity and the results are due to the presence of more carboxyl groups, revealed that the oxygen containing functional groups in the biochar are important in methylene adsorption (Lei et al., 2015a). The biochar produced from the pyrolysis of safflower seed press cake subjected for the chemical activation using zinc chloride and assessed towards the adsorption of methylene blue. The biochar content with low ash, high carbon and without sulphur offers the biomass as a good precursor for the activated carbon production. The surface area of the activated carbons increased from 249.3 to 801.5 m^2/g with the increase of activation temperature from 600 to 900 °C and impregnation ratio of 4:1. Moreover the micropore and mesopore surface areas are also increased, which are due to the tar release from the biomass with cross-linked framework structure and treatment of the zinc chloride and higher temperature (Dilek et al., 2013).

Switchgrass biochar modified using a cationic surfactant tetradecyltrimethyl ammonium bromide and used as adsorbent for the removal of the reactive red 195 A dye from aqueous solutions. The surface of activated biochar shows large number of homogeneous porous layers contributed in the enhancement of the rate of dye adsorption (Mohamed et al., 2016b). The biomass of palm bark and eucalyptus subjected as adsorbents for removal of methylene blue from aqueous solution. The major constituent of carbon in the biochars indicated the carbonaceous nature of the adsorbents. The surface area of biochars from palm bark and eucalyptus are 2.46 and 10.35 m^2/g respectively. The values of pore diameters 4.75 and 2.29 nm represented the mesoporous. The adsorption kinetic model, pseudo-second-order better described the methylene blue adsorption by the biochars. In comparison to the Freundlich adsorption isotherm model, the Langmuir model well described the methylene blue adsorption onto the biochars (Lei et al., 2013). Biochar was synthesized using pine cone by means of slow pyrolysis at 500 °C and used for the adsorption of methylene blue from aqueous phase. The adsorption of dye onto biochar represents the chemisorption process. The adsorption isotherm models of both Freundlich and Langmuir found better fitted to describe the removal of methylene blue. Thermodynamic parameters of the adsorption experimental data suggested as endothermic and spontaneous in nature (Sara et al., 2017). Waste bamboo biomass through slow pyrolysis treated at the temperature range of 400–900 °C for 1–4 h. The yield of biochar decreased with the increase of pyrolysis temperature. Noticeably the biochar yield decreased for the pyrolysis temperature increase from 400 to 500 °C, this was because of the partial gasification of lignin and hemicellulose. The high heating rates generated biochar with lower surface areas, pore volumes and reduced yields because of fast depolymerization at the surface of biochar. Bamboo biochar reported with the higher adsorption capacity towards the removal of methylene blue and acid black 172 (Mui et al., 2010; Yang et al., 2013).

The biochar activated using sulfuric acid represented higher adsorption capacity for methylene blue removal. Biochar with significant functional group and better pore structure favored the adsorption process (Wang et al., 2013). The hydrochloric acid treatment of biochar caused the formation of mesoporous structure and more negatively charge on the biochar surface, responsible the adsorption of methylene blue. The biochar had increased surface area, higher fixed carbon and oxygen content. Both the boundary layer diffusion and intra-particle diffusion controlled the adsorption of methylene blue (Mahmoud et al., 2012). Biochar obtained as byproduct during the fast pyrolysis of biomass mixture of sugarcane straw and sawdust. The controlled thermal treatment of the biochar was carried out to improve the biochar surface properties. The thermal treatment caused the organic complex biomass decomposition to micropores with graphene nanostructures. The surface area of the biochar increased from 3 m^2/g to 30, 408 and 590 m^2/g, at the thermal treatment temperatures of 400, 600 and 800 °C, respectively. The oxygen concentrations are gradually decreased with the thermal treatments due to the decomposition of oxygen surface functionalities on the biochar. The powder X-ray diffraction patterns of the biochars from thermal treatments displayed a very broad and low intensity peak around 25°, represented the amorphous carbon with weakly crystallized structures of graphene (Fernanda et al., 2017). Hickory used for the biochar preparation by slow pyrolysis with different pyrolysis temperature of 350 °C, 450 °C and 600 °C respectively. The results indicated that the pyrolysis temperature influences on the surface areas, cation-exchange capacities, zeta potential, O/C ratios and surface acidic groups (Zhuhong et al., 2016b). Table 4 summarizes the adsorption characteristics of the different biochars towards dye adsorption.

Biochar produced from the biomass of straw checked for adsorption of reactive brilliant blue and rhodamine B. The biochar was highly effective towards the both dyes removal at 3.0 pH. The dye removal by biochar occurs through electrostatic interactions and protonation at the low solution pH. The biochar presented reversed effectiveness for the adsorption of reactive brilliant blue under the same conditions. The mechanisms of the dye adsorption are due to the π–π interactions, electrostatic attraction or repulsion and intermolecular hydrogen bonding. The presence of more phenolic hydroxyls on the biochar

Table 4
Adsorption characteristics of dyes removal using different biochars.

Biochar type	Pyrolysis temperature	Residence time	Dye	Isotherm model	Kinetic model	Adsorption capacity (mg/g)	References
Canola straw	350 °C	4 h	Methyl violet	Langmuir	–	–	Xu et al., 2011
Peanut straw	350 °C	4 h	Methyl violet	Langmuir	–	256.4	
Rice hull	350 °C	4 h	Methyl violet	Langmuir	–	123.5	
Milled cotton wood	600 °C	1 h	Methylene Blue	Langmuir	–	174	Zhang et al., 2012b
Kenaf fiber	1000 °C	–	Methylene blue	Langmuir	PSO[a]	18.18	Mahmoud et al., 2012
Eucalyptus	400 °C	30 min	Methylene blue	Langmuir	PSO[a]	2.06	Lei et al., 2013
Palm bark	400 °C	30 min	Methylene blue	Langmuir	PSO[a]	2.66	
Cotton wood	600 °C	1 h	Methylene Blue	Langmuir	PSO[a]	85.0	Zhang and Gao, 2013
Rape straw	450 °C	4 h	Methylene blue	Langmuir	PSO[a]	143	Yanfang et al., 2013
Bamboo	1000 °C	–	Acid black 172	Freundlich	PSO[a]	401.88	Yang et al., 2014
Hickory chips	600 °C	1 h	Methylene Blue	Langmuir-Freundlich	Elovich	2.4	Inyang et al., 2014
Sugarcane bagasse	600 °C	1 h	Methylene Blue	Langmuir-Freundlich	PSO[a]	5.5	
Corn stalks	400 °C	2 h	Crystal violet	Langmuir	PSO[a]	278.55	Sun et al., 2015
Eichornia crassipes	300 °C	2 h	Methylene blue	Langmuir	PSO[a]	395	Yan et al., 2016
Switchgrass	450 °C	20 min	Reactive red 195 a	Langmuir	PSO[a]	1288.4	Mohamed et al., 2016b
Wheat straw	200 °C	3 h	Methylene blue	Freundlich	PSO[a]	46.6	Guoting et al., 2016
Korean cabbage	500 °C	60 min	Crystal violet	Langmuir	–	1304	Divine et al., 2017
Rice straw	500 °C	60 min	Crystal violet	Langmuir	–	620.3	
Wood chip	500 °C	60 min	Crystal violet	Langmuir	–	195.6	
Durian rind	800 °C	25 min	Congo red	–	–	87.32	Thines et al., 2017

[a] Pseudo-second-order.

surface is mainly responsible to increase π–π interactions between dye molecules and biochar graphene layers (Yuping et al., 2009). The decrease of the molar ratio H/C represents the biochar development with aromatic structures and more carbonized. The molar ratio of H/C decreased by the increase of pyrolytic temperature. Moreover, the decrease of the molar ratio O/C point out that the biochar surfaces obtained at the higher temperature became less hydrophilic in nature. Whereas the, biochar synthesized at the low pyrolysis temperature produces biochar, composed of amorphous carbon and mainly involves in the rapid adsorption process (Reguyal et al., 2017; Chen et al., 2017). The methyl violet adsorption investigated using the biochars produced from the crop residues of soybean straw, rice hull, peanut straw and canola straw. The adsorption capacity of the biomass towards the methyl violet was in the order of canola straw char > peanut straw char > soybean straw char > rice hull char. The analysis of the results of zeta potential, Fourier transforms infrared photoacoustic spectroscopy spectra, adsorption isotherms and influence of ionic strength revealed that the methyl violet removal by biochars based on electrostatic attraction, methyl violet and the functional groups (−COO^- and phenolic−OH) interactions and surface precipitation. The electrostatic interaction between the biochar derived from crop residue and methyl violet increased with the increase of solution pH because of the biochar functional group phenolic −OH dissociation, consequent to the raised net negative charge on the biochar surface (Xu et al., 2011). The initial solution pH and ionic strength affect the adsorption of dye onto the biochar (Mahmoud et al., 2012). At the higher solution pH, the electrostatic attraction exhibited between the methylene blue and citric acid modified biochar from water hyacinth. This caused the increase of the adsorption of methylene blue onto the biochar. The results revealed that the mechanism of electrostatic attraction mainly involved in the methylene blue removal (Yan et al., 2016).

5.3. Miscellaneous pollutants removal

Apart from the heavy metals and dyes removal by biochar, the other wastewater pollutants like pharmaceuticals, pesticides/herbicides, Phenols are also reported on the adsorptive removal using biochar (Chanil et al., 2013; Matthew et al., 2015; Sherif et al., 2014; Abhishek et al., 2017; Xiao and Pignatello, 2015; Yanxue et al., 2013; Mubarik et al., 2016). The influence of co-existence of organic matter and salts on the removal of ibuprofen and sulfamethoxazole examined using biochars. The biochar uptake capacity towards the removal of pharmaceuticals affected by their physical and chemical characteristic features such as surface area, pore volume, ash content, hydrophobicity, π-energy, charge and pharmaceuticals speciation (Lu et al., 2017). The adsorption parameter of the values of solution pH had a little affect on the removal of carbamazepine and tetracycline using biochars (Shan et al., 2016). The adsorption of carbamazepine performed using biochar derived from peanut shell biomass at different pyrolysis temperatures. The adsorption mechanisms of carbamazepine onto biochar were mainly due to the hydrophobic and π-π interactions. The minerals like calcium carbonate, potassium aluminate and quartz in the biochar are the chief factors for the rapid adsorption of carbamazepine occurred through the formation of hydrogen bonds between carbamazepine and hydroxyl on the minerals surface in biochar (Jian et al., 2017). The biomass of *Sicyos angulatus* subjected for the biochar production and then steam activated, further tested on the adsorption of sulfamethazine from aqueous solution. The highest adsorption capacity observed at the solution pH of 3.0. Electrostatic interaction mainly contributed in the adsorption of sulfamethazine, in addition other mechanisms like hydrogen bond, hydrophobic and π-π interactions are also involved (Rajapaksha et al., 2015)

Biomass from eucalyptus bark, corncob, bamboo chips, rice husk, rice straw and acid treated rice straw were used as precursor for the biochar production. The biochars were assessed towards the adsorption of atrazine and imidacloprid from aqueous solutions. Comparatively, rice straw showed higher removal efficiency towards the removal of both atrazine and imidacloprid. Moreover, the phosphoric acid modified rice straw biochar reported with enhanced adsorption. The biochar factors like pore diameter, pH, aromaticity, polarity and weak acid fraction affect the adsorption of pesticide (Abhishek et al., 2017). Biochar from almond shells was produced through slow pyrolysis, further subjected for steam activation. The surface area of the activated biochar was 344 m^2/g. The maximum adsorption capacity of biochar towards the removal of dibromochloropropane was 102 mg/g (Klasson et al., 2013). Biochar from the green waste biomass evaluated for the

adsorption of atrazine and simazine. The better adsorption of atrazine and simazine occurred at the low solution pH. The biochar adsorption affinity towards atrazine and simazine removal increased with the decrease of solid/solution ratio. In the binary adsorption system, competitive pattern of pesticides binding on the biochar occurred and caused the decrease in adsorption capacity from 435 to 286 mg/kg towards atrazine removal and from 514 to 212 mg/kg towards simazine removal (Wei et al., 2010). Rice husk biochar was examined for the adsorption of the metolachlor. The pyrolysis temperature had direct influence on the biochar surface area. At the highest pyrolysis temperature of 750 °C, the biochar produced with better surface area of 53.08 m^2/g. The biochars obtained from different pyrolysis temperatures presents specific mechanisms for the adsorption of metolachlor. The biochar produced at the low pyrolytic temperature, the hydrogen bonds is the dominants and in the higher pyrolytic temperature produced biochar, pore filling prevails (Lan et al., 2017). The feedstock biomass of peanut shell and wheat straw utilized for biochar production and tested for the adsorption of atrazine, 17α-ethinyl estradiol and phenanthrene. The planar organic pollutant phenanthrene gets easily adsorbed onto the biochars of peanut shell and wheat straw. The stronger aliphaticity and polarity property of wheat straw was due to the higher ratios of H/C and (O + N)/C, caused the higher affinity towards atrazine and phenanthrene. The biochar from peanut shell has larger surface area of 19.7 m^2/g and this attributes to the higher adsorption capacity towards 17α-ethinyl estradiol removal (Jiangmin et al., 2016).

The biomass of rice husk and corncob used for the preparation of biochar, performed at a particular temperature and with varying residence times. Biochar obtained at the residence time of 1.6 s showed higher phenol adsorption capacity of 589 mg/g. The phenol adsorption occurs through the interaction of acid–base and hydrogen bonding (Liu et al., 2011). The adsorption of 2, 4-dichlorophenol was examined using wheat husks biochar. The better fit of equilibrium data with both Langmuir and Freundlich isotherm model represented surface and multilayer adsorption process. The adsorption mechanisms of electrostatic interactions are mainly dependent on the solution pH. The higher concentrations of cations such as calcium and potassium promote the adsorption of 2,4-dichlorophenol onto biochar (Dimitrios et al., 2017). Sugarcane baggase biochar prepared through heat treatment at 673 K and used for the adsorption of 2,4,6-trichlorophenol. Biochar consists of highly porous structure with the shape of deep well cylindrical tubes, 50.47% fixed carbon and surface area of about 361.77 m^2/g. The biochar consists of different functional moieties (Mubarik et al., 2016). The adsorption capacity of acid washed reed biochar showed higher adsorption capacity towards pentachlorophenol removal than the unmodified reed biochar. The inorganic element in the biochars offer hydrophilic nature and thereby shows the negligible or negative influence on the adsorption of pentachlorophenol. The adsorption mechanism of pentachlorophenol was mainly due to the π–π and hydrophobic interactions (Peng et al., 2016).

6. Conclusions

The recent studies on the lignocellulosic biomass as suitable precursor for the production of biochar have been reviewed. The thermochemical conversion of lignocellulosic biomass by pyrolysis offered as an appropriate process for the production of biochar. The growing interest on the biochar synthesis resulted in the exploration of sustainable feedstock source from lignocellulosic biomass such as agricultural residues, forestry residues and herbaceous biomass. The feedstock from agricultural residues is distributed copious in the agricultural practicing, developing country like India. The conversion of the lignocellulose components into various pyrolysis products depends on the biomass composition and pyrolysis conditions. The lignocellulosic biomass with the high lignin content favors the production of biochar. The pyrolysis parameters such as the temperature, heating rate and residence time have direct influence on the production of biochar. The biochar modification through different activation methods reported with the enhanced physico-chemical properties including the specific surface area, functional group distribution. The biochar with the potential characteristics features explored by many researchers subjected for the application as promising adsorbents for the removal of toxic heavy metals and dyes from the aqueous solutions. The Langmuir adsorption isotherm model and pseudo-second-order kinetic model are found to be best that described the adsorption data of heavy metal and dye removal using biochar.

More research is needed on the optimization techniques for the maximum biochar production yield, cost-factor analysis for biochar production, multi-component study, dynamic investigation, modeling and biochar regeneration. Followed with the simulated system, the biochar efficiency needs to be examined using the real time industrial effluents. The employment of spent biochar after proper desorption towards the application in contaminated soil remediation as well may offers the benefits of conservation agricultural practices.

Acknowledgements

Financial support from the Science and Engineering Research Board (SERB), India (File No. ECR/2017/003397) is acknowledged. The authors would like to thank SASTRA University and National Institute of Technology Rourkela for providing the research facility.

References

Abdolali, A., Guo, W.S., Ngo, H.H., Chen, S.S., Nguyen, N.C., Tung, K.L., 2014. Typical lignocellulosic wastes and by-products for biosorption process in water and wastewater treatment: a critical review. Bioresour. Technol 160, 57–66.
Abhishek, M., Neera, S., Purakayastha, T.J., 2017. Characterization of pesticide sorption behaviour of slow pyrolysis biochars as low cost adsorbent for atrazine and imidacloprid removal. Sci. Total Environ. 577, 376–385.
Adel, U., Abdulazeem, S., Ming, Z., Meththika, V., Mahtab, A., Abdullah, A.F., Yong, S.O., Adel, A., Mohammad, A.W., 2016. Sorption process of date palm biochar for aqueous Cd(II) removal: efficiency and mechanisms. Water Air Soil Pollut. Focus. 227, 449–464.
Agrafioti, E., Kalderis, D., Diamadopoulos, E., 2014. Ca and Fe modified biochars as adsorbents of arsenic and chromium in aqueous solutions. J. Environ. Manage. 146, 444–450.
Ahmad, M., Lee, S.S., Dou, X., Mohan, D., Sung, J.K., Yang, J.E., Ok, Y.S., 2012. Effects of pyrolysis temperature on soybean stover- and peanut shell-derived biochar properties and TCE adsorption in water. Bioresour. Technol. 118, 536–544.
Ahmed, M.J., 2016. Alication of agricultural based activated carbons by microwave and conventional activations for basic dye adsorption: review. J. Environ. Chem. Eng. 4, 89–99.
Akar, S.T., Ozcan, A.S., Akar, T., Ozcan, A., Kaynak, Z., 2009. Biosorption of a reactive textile dye from aqueous solutions utilizing an agro-waste. Desalination 249, 757–761.
Aleksandra, B., Patryk, O., Ryszard, D., 2015. Application of laboratory prepared and commercially available biochars to adsorption of cadmium, copper and zinc ions from water. Bioresour. Technol. 196, 540–549.
Alen, R., Kuoala, E., Oesch, P., 1996. Formation of the main degradation compound, groups from wood and its components during pyrolysis. J. Anal. Appl. Pyrolysis 36, 137–148.
Andres, A.C., 2016. Reaction mechanisms and multi-scale modelling of lignocellulosic biomass pyrolysis. Prog. Energy Combust. Sci. 53, 41–79.
Anna, T., Peter, A.J., Anker, D.J., Markus, S., Hartmut, S., Peter, G., 2015. Influence of fast pyrolysis conditions on yield and structural transformation of biomass chars. Fuel Process. Technol. 140, 205–214.
Antal, M.J., Gronli, M., 2003. The art, science, and technology of charcoal production. Ind. Eng. Chem. Res. 42, 1619–1640.
Antonio, G.C., Massimo, P., Alessia, S., Pellegrino, C., 2014. Effect of pruning-derived biochar on heavy metals removal and water dynamics. Biol. Fert. Soils. 50, 1211–1222.
Ayman, A.I., Yahya, S.A., Mohammad, A.A., Amal, A.M.O., 2014. Studying competitive sorption behavior of methylene blue and malachite green using multivariate calibration. Chem. Eng. J. 240, 554–564.
Azargohar, R., Dalai, A.K., 2008. Steam and KOH activation of biochar: experimental and modeling studies. Microporous Mesoporous Mater. 110, 413–421.
Azargohar, R., Jacobson, K.L., Powell, E.E., Dalai, A.K., 2013. Evaluation of properties of fast pyrolysis products obtained, from Canadian waste biomass. J. Anal. Appl. Pyrolysis 104, 330–340.
Bach, M.T., 2007. Impact of Surface Chemistry on Adsorption: Tailoring of Activated Carbon. University of Florida, pp. 132.
Baig, S.A., Zhu, J., Muhammad, N., Sheng, T., Xu, X., 2014. Effect of synthesis methods on

magnetic Kans grass biochar for enhanced As (III, V) adsorption from aqueous solutions. Biomass Bioenergy 71, 299–310.
Basu, P., 2010. Biomass Gasification and Pyrolysis: Practical Design and Theory. Elsevier, Burlington, MA.
Boateng, A.A., 2007. Characterization and thermal conversion of charcoal derived from fluidized-bed fast pyrolysis oil production of switchgrass. Ind. Eng. Chem. Res. 46, 8857–8862.
Bouchelta, C., Medjram, M.S., Zoubida, M., Chekkat, F.A., Ramdane, N., Bellat, J.P., 2012. Effects of pyrolysis conditions on the porous structure development of date pits activated carbon. J. Anal. Appl. Pyrolysis 94, 215–222.
Brassard, P., Godbout, S., Raghavan, V., 2016. Soil biochar amendment as a climate change mitigation tool: key parameters and mechanisms involved. J. Environ. Manage. 181, 484–497.
Bridgwater, A.V., 2012. Review of fast pyrolysis of biomass and product upgrading. Biomass Bioenergy 38, 68–94.
Burhenne, L., Aicher, T., 2014. Benzene removal over a fixed bed of wood char: the effect of pyrolysis temperature and activation with CO_2 on the char reactivity. Fuel Process. Technol. 127, 140–148.
Butler, E., Devlin, G., Meier, D., Mc Donnell, K., 2013. Fluidised bed pyrolysis of lignocellulosic biomasses and comparison of bio-oil and micropyrolyser pyrolysate by GC/MS-FID. J. Anal. Appl. Pyrolysis 103, 96–101.
Cao, X., Harris, W., 2010. Properties of dairy-manure-derived biochar pertinent to its potential use in remediation. Bioresour. Technol. 101, 5222–5228.
Caprariis, B., Santarelli, M.L., Scarsella, M., Herce, C., Verdone, N., De Filiis, P., 2015. Kinetic analysis of biomass pyrolysis using a double distributed activation energy model. J. Therm. Anal. Calorim. 121, 1403–1410.
Caprariis, B., Filiis, P.D., Hernandez, D., Petrucci, E., Petrullo, A., Scarsella, A., Turchi, M., 2017. Pyrolysis wastewater treatment by adsorption on biochars produced by poplar biomass. J. Environ. Manage. 197, 231–238.
Chang, M.P., Jonghun, H., Kyoung, H.C., Yasir, A.J.A.H., Namguk, H., Jiyong, H., Yeomin, Y., 2017. Influence of solution pH, ionic strength, and humic acid on cadmium adsorption onto activated biochar: experiment and modeling. J. Ind. Eng. Chem. 48, 186–193.
Chanil, J., Junyeong, P., Kwang, H.L., Sunkyu, P., Jiyong, H., Namguk, H., Jeill, O., Soyoung, Y., Yeomin, Y., 2013. Adsorption of selected endocrine disrupting compounds and pharmaceuticals on activated biochars. J. Hazard. Mater. 263, 702–710.
Chao, Z., Baoqing, S., Wenzhong, T., Yaoyao, Z., 2017. Comparison of cadmium and lead sorption by *Phyllostachys pubescens* biochar produced under a low-oxygen pyrolysis atmosphere. Bioresour. Technol. 238, 352–360.
Chen, B., Chen, Z., 2009. Sorption of naphthalene and 1-naphthol by biochars of orange peels with different pyrolytic temperatures. Chemosphere 76, 127–133.
Chen, B., Chen, Z., Lv, S., 2011a. A novel magnetic biochar efficiently sorbs organic pollutants and phosphate. Bioresour. Technol. 102, 716–723.
Chen, B., Zhou, D., Zhu, L., 2008. Transitional adsorption and partition of nonpolar and polar aromatic contaminants by biochars of pine needles with different pyrolytic temperatures. Environ. Sci. Technol. 42, 5137–5143.
Chen, G., Andries, J., Luo, Z., Spliethoff, H., 2003. Biomass pyrolysis/gasification for product gas production: the overall investigation of parametric effects. Energy Convers. Manage. 44, 1875–1884.
Chen, J., Zhang, D., Zhang, H., Ghosh, S., Pan, B., 2017. Fast and slow adsorption of carbamazepine on biochar as affected by carbon structure and mineral composition. Sci. Total Environ. 579, 598–605.
Chen, T., Zhang, Y., Wang, H., Lu, W., Zhou, Z., Zhang, Y., Ren, L., 2014. Influence of pyrolysis temperature on characteristics and heavy metal adsorptive performance of biochar derived from municipal sewage sludge. Bioresour. Technol. 164, 47–54.
Chen, W.H., Lu, K.M., Tsai, C.M., 2012. An experimental analysis on property and structure variations of agricultural wastes undergoing torrefaction. Appl. Energy 100, 318–325.
Chen, X., Chen, G., Chen, L., Chen, Y., Lehmann, J., McBride, M.B., Hay, A.G., 2011b. Adsorption of coer and zinc by biochars produced from pyrolysis of hardwood and corn straw in aqueous solution. Bioresour. Technol. 102, 8877–8884.
Ci, F., Tao, Z., Rongfeng, J., Shubiao, W., Haiyu, N., Yingcai, W., 2015. Phosphorus recovery from biogas fermentation liquid by Ca–Mg loaded biochar. J. Environ. Sci. China (China) 29, 106–114.
Collard, F.X., Blin, J., Bensakhria, A., Valette, J., 2012. Influence of impregnated metal on the pyrolysis conversion of biomass constituents. J. Anal. Appl. Pyrolysis 95, 213–226.
Cope, C.O., Webster, D.S., Sabatini, D.A., 2014. Arsenate adsorption onto iron oxide amended rice husk char. Sci. Total Environ. 488, 554–561.
Cui, Q., Ningbo, G., Qingbin, S., 2016. Pyrolysis of biomass components in a TGA and a fixed-bed reactor: thermochemical behaviors, kinetics, and product characterization. J. Anal. Appl. Pyrolysis 121, 84–92.
Angin, D., 2013. Effect of pyrolysis temperature and heating rate on biochar obtained from pyrolysis of safflower seed press cake. Bioresour. Technol. 128, 593–597.
Damartzis, T., Vamvuka, D., Sfakiotakis, S., Zabaniotou, A., 2011. Thermal degradation studies and kinetic modeling of cardoon (*Cynara cardunculus*) pyrolysis using thermogravimetric analysis (TGA). Bioresour. Technol. 102, 6230–6238.
Daniel, N., Henrik, T., Arlindo, M., Luis, T., Alberto, G.B., 2011. Characterization and prediction of biomass pyrolysis products. Prog. Energy Combust. Sci. 37, 611–630.
Dengyu, C., Xinzhi, Y., Chao, S., Xiaoli, P., Jing, H., Yanjun, L., 2016a. Effect of pyrolysis temperature on the chemical oxidation stability of bamboo biochar. Bioresour. Technol. 218, 1303–1306.
Dengyu, C., Yanjun, L., Kehui, C., Min, L., Hongyan, L., Bin, L., 2016b. Pyrolysis polygeneration of poplar wood: effect of heating rate and pyrolysis temperature. Bioresour. Technol. 218, 780–788.
Di, B.C., 2008. Modeling chemical and physical processes of wood and biomass pyrolysis. Prog. Energy Combust. Sci. 34, 47–90.
Dias, D., Lapa, N., Bernardo, M., Godinho, D., Fonseca, I., Miranda, M., Pinto, F., Lemos, F., 2017. Properties of chars from the gasification and pyrolysis of rice waste streams towards their valorization as adsorbent materials. Waste Manag. 65, 186–194.
Dilek, A., Esra, A., Tijen, E.K., 2013. Influence of process parameters on the surface and chemical properties of activated carbon obtained from biochar by chemical activation. Bioresour. Technol. 148, 542–549.
Dimitrios, K., Berkant, K., Sema, A., Esra, K., Belgin, G., 2017. Adsorption of 2,4-dichlorophenol on paper sludge/wheat husk biochar: Process optimization and comparison with biochars prepared from wood chips, sewage sludge and hog fuel/demolition waste. J. Environ. Chem. Eng. 5, 2222–2231.
Divine, D.S., Patrick, B., Seung, H.W., 2017. Highly efficient adsorption of cationic dye by biochar produced with Korean cabbage waste. Bioresour. Technol. 224, 206–213.
Dongdong, F., Yijun, Z., Yu, Z., Zhibo, Z., Linyao, Z., Jianmin, G., Shaozeng, S., 2017. Synergetic effects of biochar structure and AAEM species on reactivity of H_2O-activated biochar from cyclone air gasification. Int. J. Hydrogen Energy 42, 16045–16053.
Dorez, G., Ferry, L., Sonnier, R., Taguet, A., Lopez-Cuesta, J.M., 2014. Effect of cellulose, hemicellulose and lignin contents on pyrolysis and combustion of natural fibers. J. Anal. Appl. Pyrolysis 107, 323–331.
Ehsan, D., Arya, V., Ali, N., Mika, S., Amit, B., 2017. A comparative study of methylene blue biosorption using different modified brown, red and green macroalgae – effect of pretreatment. Chem. Eng. J. 307, 435–446.
Eom, I.Y., Kim, J.Y., Kim, T.S., Lee, S.M., Choi, D., Choi, I.G., Choi, J.W., 2012. Effect of essential inorganic metals on primary thermal degradation of lignocellulosic biomass. Bioresour. Technol. 104, 687–694.
FAOSTAT, 2014. Food and Agriculture Organization of the United Nations, Rome.
Fassinou, W.F., Vande Steene, L., Toure, S., Volle, G., Girard, P., 2009. Pyrolysis of Pinus pinaster in a two-stage gasifier: influence of processing parameters and thermal cracking of tar. Fuel Process. Technol. 90, 75–90.
Fernanda, G.M., Igor, T.C., Ricardo, R.S., Juliana, C.T., Rochel, M.L., 2017. Tuning the surface properties of biochar by thermal treatment. Bioresour. Technol. 246, 28–33.
Fisher, T., Hajaligol, M., Waymack, B., Kellogg, D., 2002. Pyrolysis behavior and kinetics of biomass derived materials. J. Anal. Appl. Pyrolysis 62, 331–349.
Fristak, V., Pipiska, M., Lesny, J., Soja, G., Friesl-Hanl, W., Packova, A., 2015. Utilization of biochar sorbents for Cd^{2+}, Zn^{2+}, and Cu^{2+} ions separation from aqueous solutions: comparative study. Environ. Monit. Assess. 187, 4093.
Fuat, G., Hasan, S., Gulbahar, A.S., Filiz, K., Cumali, Y., 2017. Optimal oxidation with nitric acid of biochar derived from pyrolysis of weeds and its alication in removal of hazardous dye methylene blue from aqueous solution. J. Clean. Prod. 144, 260–265.
Gallezot, P., 2012. Conversion of biomass to selected chemical products. Chem. Soc. Rev. 41, 1538–1558.
Gang, C., Jing, Z., Fangyuan, C., Xudong, D., Dandan, Z., Ni, L., Min, W., Bo, P., Christian, E.W.S., 2017. Physi-chemical and sorption properties of biochars prepared from peanut shell using thermal pyrolysis and microwave irradiation. Environ. Pollut. 227, 372–379.
George, T., Simona, M., Katerina, S., Peter, T., Tony, S., 2016. Mechanochemical and chemical activation of lignocellulosic material to prepare powdered activated carbons for adsorption alications. Powder Technol. 299, 41–50.
Guohua, L., Qiang, X., Xiaobo, D., Jing, Y., Lauren, S.P., Wang, G.G., Fusheng, W., 2016. Effect of protective gas and pyrolysis temperature on the biochar produced from three plants of Gramineae: physical and chemical characterization. Waste Biomass Valor. 7, 1469–1480.
Guoting, L., Weiyong, Z., Chunyu, Z., Shen, Z., Lili, L., Lingfeng, Z., Weigao, Z., 2016. Effect of a magnetic field on the adsorptive removal of methylene blue onto wheat straw biochar. Bioresour. Technol. 206, 16–22.
Haiping, Y., Rong, Y., Hanping, C., Dong, H.L., Chuguang, Z., 2007. Characteristics of hemicellulose, cellulose and lignin pyrolysis. Fuel 86, 1781–1788.
Hao, W., Bjorkman, E., Lilliestrale, M., Hedin, N., 2013. Activated carbons prepared from hydrothermally carbonized waste biomass used as adsorbents for CO_2. Appl. Energy 112, 526–532.
Helena, R., Agnieszka, C., Dagmar, J., Veronika, S., Jaroslav, F., 2015. Effect of temperature on the enrichment and volatility of 18 elements during pyrolysis of biomass, coal, and tires. Fuel Process. Technol. 131, 330–337.
Hoda, S., Pouya, S.R., Wan, M.A.W.D., 2016. Catalytic hydrodeoxygenation of simulated phenolic bio-oil to cycloalkanes and aromatic hydrocarbons over bifunctional metal/acid catalysts of Ni/HBeta, Fe/HBeta and NiFe/HBeta. J. Ind. Eng. Chem. 35, 268–276.
Hongbo, L., Xiaoling, D., Evandro, B.S., Letuzia, M.O., Yanshan, C., Lena, Q.M., 2017. Mechanisms of metal sorption by biochars: biochar characteristics and modifications. Chemosphere 178, 466–478.
Hosoya, T., Kawamoto, H., Saka, S., 2007. Pyrolysis behaviors of wood and its constituent polymers at gasification temperature. J. Anal. Appl. Pyrolysis 78, 328–336.
Hsu, N.H., Wang, S.L., Lin, Y.C., Sheng, G.D., Lee, J.F., 2009. Reduction of Cr(VI) by crop-residue-derived black carbon. Environ. Sci. Technol. 43, 8801–8806.
Huff, M.D., Kumar, S., Lee, J.W., 2014. Comparative analysis of pinewood, peanut shell, and bamboo biomass derived biochars produced via hydrothermal conversion and pyrolysis. J. Environ. Manage. 146, 303–308.
Inyang, M., Gao, B., Ding, W., Pullammanaallil, P., Zimmerman, A.R., Cao, X., 2011. Enhanced lead sorption by biochar derived from anaerobically digested sugarcane bagasse. Sep. Sci. Technol. 46, 1950–1956.
Inyang, M., Gao, B., Zimmerman, A., Zhang, M., Chen, H., 2014. Synthesis, characterization, and dye sorption ability of carbon nanotube–biochar nanocomposites. Chem. Eng. J. 236, 39–46.
Islam, M.A., Benhouria, A., Asif, M., Hameed, B.H., 2015a. Methylene blue adsorption on factory-rejected tea activated carbon prepared by conjunction of hydrothermal

carbonization and sodium hydroxide activation processes. J. Taiwan Inst. Chem. Eng. 52, 57–64.
Islam, M.A., Auta, M., Kabir, G., Hameed, B.H., 2016. A thermogravimetric analysis of the combustion kinetics of karanja (*Pongamia pinnata*) fruit hulls char. Bioresour. Technol. 200, 335–341.
Islam, M.A., Tan, I.A.W., Benhouria, A., Asif, M., Hameed, B.H., 2015b. Mesoporous and adsorptive properties of palm date seed activated carbon prepared via sequential hydrothermal carbonization and sodium hydroxide activation. Chem. Eng. J. 270, 187–195.
Jain, M., Garg, V.K., Kadirvelu, K., Sillanpa, M., 2016. Adsorption of heavy metals from multi-metal aqueous solution by sunflower plant biomass-based carbons. Int. J. Environ. Sci. Technol. (Tehran) 13, 493–500.
Jersson, P., Sergio, C., 2015. Production of silicon compounds and fulvic acids from cotton wastes biochar using chemical depolymerization. Ind. Crops Prod. 67, 270–280.
Jian, C., Di, Z., Huang, Z., Saikat, G., Bo, P., 2017. Fast and slow adsorption of carbamazepine on biochar as affected by carbon structure and mineral composition. Sci. Total Environ. 579, 598–605.
Jiangmin, Z., Hualin, C., Weilin, H., Joselito, M.A., Shimei, G., 2016. Sorption of atrazine, 17α-Estradiol, and phenanthrene on wheat straw and peanut shell biochars. Water Air Soil Pollut. 227, 7–19.
Jin, H., Capareda, S., Chang, Z., Gao, J., Xu, Y., Zhang, J., 2014. Biochar pyrolytically produced from municipal solid wastes for aqueous As(V) removal: adsorption property and its improvement with KOH activation. Bioresour. Technol. 169, 622–629.
Jing, R., Nan, L., Lin, Z., Lei, L., 2017. Pretreatment of raw biochar and phosphate removal performance of modified granular Iron/Biochar. Tianjin 23, 340–350.
Jingge, S., Jiachang, P., Mingzhu, Z., Yingrong, W., Wenhong, L., Qianjiahua, L., 2016. Chromium removal using magnetic biochar derived from herb-residue. J. Taiwan Inst. Chem. Eng. 68, 289–294.
Jingjian, P., Jun, J., Renkou, X., 2013. Adsorption of Cr(III) from acidic solutions by crop straw derived biochars. J. Environ. Sci. China (China) 25, 1957–1965.
Jinshuai, Y., Yicheng, Z., Yongdan, L., 2014. Utilization of corn cob biochar in a direct carbon fuel cell. J. Power Sour. 270, 312–317.
Jong, H.P., Yong, S.O., Seong, H.K., Se, W.K., Ju, S.C., Jong, S.H., Ronald, D.D., Dong, C.S., 2015. Characteristics of biochars derived from fruit tree pruning wastes and their effects on lead adsorption. J. Korean Soc. Appl. Biol. Chem. 58, 751–760.
Joyce, S.C., Suzanne, B., Ted, M.K., Joseph, M., Cliff, T.J., Brad, J., 2017. Initial biochar properties related to the removal of As, Se, Pb, Cd, Cu, Ni, and Zn from an acidic suspension. Chemosphere 170, 216–224.
Kangning, X., Chuke, Z., Xiaomin, D., Weifang, M., Chengwen, W., 2017. Optimizing the Modification of Wood Waste Biochar Via Metal Oxides to Remove and Recover Phosphate From Human Urine. Environ. Geochem. Healthhttps://doi.org/10.1007/s10653-017-9986-6.
Karaosmanoglu, F., Ergudenler, A.I., Sever, A., 2000. Biochar from the straw–stalk of rapeseed plant. Energy Fuels 14, 336–339.
Katerina, B., Jirina, S., Miloslav, L., Tereza, K., Miroslav, P., Pavel, T., 2017. Biochar physicochemical parameters as a result of feedstock material and pyrolysis temperature: predictable for the fate of biochar in soil? Environ. Geochem. Health. https://doi.org/10.1007/s10653-017-0004-9.
Keiluweit, M., Nico, P.S., Johnson, M.G., Kleber, M., 2010. Dynamic molecular structure of plant biomass-derived black carbon (biochar). Environ. Sci. Technol. 44, 1247–1253.
Khan, A., Rashid, A., Younas, R., 2015. Adsorption of reactive Black-5 by pine needles biochar produced via catalytic and non-catalytic pyrolysis. Arab. J. Sci. Eng. 40, 1269–1278.
Khare, P., Dilshad, U., Rout, P.K., Yadav, V., Jain, S., 2017. Plant refuses driven biochar: application as metal adsorbent from acidic solutions. Arab. J. Chem. 10, S3054–S3063.
Kifayat, U., Vinod, K.S., Sunil, D., Giacobbe, B., Mushtaq, A., Sofia, S., 2015. Assessing the lignocellulosic biomass resources potential in developing countries. A critical review. Renew. Sust. Energ. Rev. 51, 682–698.
Kim, P., Johnson, A., Edmunds, C.W., Radosevich, M., Vogt, F., Rials, T.G., Labbe, N., 2011. Surface functionality and carbon structures in lignocellulosic-derived bio-chars produced by fast pyrolysis. Energy Fuels 25, 4693–4703.
Kim, W.K., Shim, T., Kim, Y.S., Hyun, S., Ryu, C., Park, Y.K., Jung, J., 2013. Characterization of cadmium removal from aqueous solution by biochar produced from a giant Miscanthus at different pyrolytic temperatures. Bioresour. Technol. 138, 266–270.
Kim, Y.M., Jae, J., Myung, S., Sung, B.H., Dong, J.I., Park, Y.K., 2016. Investigation into the lignin decomposition mechanism by analysis of the pyrolysis product of Pinus radiate. Bioresour. Technol. 219, 371–377.
Klasson, K.T., Ledbetter, C.A., Uchimiya, M., Lima, I.M., 2013. Activated biochar removes 100% dibromochloropropane from field well water. Environ. Chem. Lett. 11, 271–275.
Ko, J.H., Kwak, Y.H., Yoo, K.S., Jeon, J.K., Park, S.H., Park, Y.K., 2011. Selective catalytic reduction of NO_x using RDF char and municipal solid waste char based catalyst. J Mater. Cycles Waste. 13, 173–179.
Kong, S.H., Loh, S.K., Bachmann, R.T., Rahim, S.A., Salimon, J., 2014. Biochar from oil palm biomass: a review of its potential and challenges. Renew. Sust. Energ. Rev. 39, 729–739.
Kostas, K., Dimitra, Z., Ioannis, P., Despina, V., Georgios, B., 2015. Assessment of pistachio shell biochar quality and its potential for adsorption of heavy metals. Waste Biomass Valorization 6, 805–816.
Kowalski, T., Ludwig, C., Wokaun, A., 2007. Qualitative evaluation of alkali release during the pyrolysis of biomass. Energy Fuel. 21, 3017–3022.
Kwapinski, W., Byrne, C.M.P., Kryachko, E., Wolfram, P., Adley, C., Leahy, J.J., Novotny, E.H., Hayes, M.H.B., 2010. Biochar from biomass and waste. Waste Biomass Valor. 1, 177–189.
Lan, W., Yufen, H., Yanliang, L., Lianxi, H., Nyo, N.M., Qing, H., Zhongzhen, L., 2017. Biochar characteristics produced from rice husks and their sorption properties for the acetanilide herbicide metolachlor. Environ. Sci. Pollut. Res. Int. 24, 4552–4561.
Lange, J.P., 2007. Lignocellulose conversion: an introduction to chemistry, process and economics. Biofuel. Bioprod. Bior. 1, 39–48.
Lee, J.W., Kidder, M., Evans, B.R., Paik, S., Buchanan Iii, A., Garten, C.T., Brown, R.C., 2010. Characterization of biochars produced from cornstovers for soil amendment. Environ. Sci. Technol. 44, 7970–7974.
Lee, S.J., Park, J.H., Ahn, Y.T., Chung, J.W., 2015. Comparison of heavy metal adsorption by Peat Moss and peat moss-derived biochar produced under different carbonization conditions. Water Air Soil Pollut. 226, 9–19.
Lehmann, J., 2007. Bio-energy in the black. Front. Ecol. Environ. 5, 381–387.
Lei, S., Dongmei, C., Shungang, W., Zebin, 2015a. Performance, kinetics, and equilibrium of methylene blue adsorption on biochar derived from eucalyptus saw dust modified with citric, tartaric, and acetic acids. Bioresour. Technol. 198, 300–308.
Lei, S., Shungang, W., Wensui, L., 2013. Biochars prepared from anaerobic digestion residue, palm bark, and eucalyptus for adsorption of cationic methylene blue dye: characterization, equilibrium, and kinetic studies. Bioresour. Technol. 140, 406–413.
Lei, Z., Hanwu, L., Lu, W., Gayatri, Y., Xuesong, Z., Yi, W., Yupeng, L., Di, Y., Shulin, C., Birgitte, A., 2015b. Biochar of corn stover: microwave-assisted pyrolysis condition induced changes in surface functional groups and characteristics. J. Anal. Appl. Pyrolysis 115, 149–156.
Leng, L., Yuan, X., Huang, H., Wang, H., Wu, Z., Fu, L., Peng, X., Chen, X., Zeng, G., 2015. Characterization and alication of bio-chars from liquefaction of microalgae, lignocellulosic biomass and sewage sludge. Fuel Process. Technol. 129, 8–14.
Li, M., Liu, Q., Guo, L., Zhang, Y., Lou, Z., Wang, Y., Qian, G., 2013. Cu(II) removal from aqueous solution by Spartina alterniflora derived biochar. Bioresour. Technol. 141, 83–88.
Li, Y., Yu, S., Strong, J., Wang, H., 2012. Are the biogeochemical cycles of carbon, nitrogen, sulfur, and phosphorus driven by the "FeIII-FeII redox wheel" in dynamic redox environments? J. Soils Sediments 12, 683–693.
Lillo, R.M.A., Cazorla, A.D., Linares, S.A., 2003. Understanding chemical reactions between carbons and NaOH and KOH: an insight into the chemical activation mechanism. Carbon 41, 267–275.
Lina, L., Weiwen, Q., Di, W., Zhengguo, S., Henry, W.C., 2017. Arsenic removal in aqueous solution by a novel Fe-Mn modified biochar composite: characterization and mechanism. Ecotoxicol. Environ. Saf. 144, 514–521.
Linson, L., Tarek, R., Kumar, D., Satinder, K.B., Antonio, A.R., Mausam, V., Rao, Y.S., Jose, R.V., 2016. Adsorption of methylene blue on biochar microparticles derived from different waste materials. Waste Manage. 49, 537–544.
Liu, Q., Wang, S.R., Zheng, Y., Luo, Z.Y., Cen, K.F., 2008. Mechanism study of wood lignin pyrolysis by using TG-FTIR analysis. J. Anal. Appl. Pyrolysis 82, 170–177.
Liu, S., Xu, W.H., Liu, Y.G., Tan, X.F., Zeng, G.M., Li, X., Liang, J., Zhou, Z., Yan, Z.L., Cai, X.X., 2017. Facile synthesis of Cu(II) impregnated biochar with enhanced adsorption activity for the removal of doxycycline hydrochloride from water. Sci. Total Environ. 592, 546–553.
Liu, W.J., Zeng, F.X., Jiang, H., Zhang, X.S., 2011. Preparation of high adsorption capacity bio-chars from waste biomass. Bioresour. Technol. 102, 8247–8252.
Liu, Z., Zhang, F.S., Wu, J., 2010. Characterization and alication of chars produced from pinewood pyrolysis and hydrothermal treatment. Fuel. 89, 510–514.
Lou, K., Rajapaksha, A.U., Ok, Y.S., Chang, S.X., 2016. Sorption of copper(II) from synthetic oil sands process-affected water (OSPW) by pine sawdust biochars: effects of pyrolysis temperature and steam activation. J. Soils Sediments 16, 2081–2089.
Loukia, H., Melpomeni, P., Ioannis, P., 2014. Activated biochar derived from cactus fibres – Preparation, characterization and alication on Cu(II) removal from aqueous solutions. Bioresour. Technol. 159, 460–464.
Lu, G.Q., Low, J.C.F., Liu, C.Y., Lua, A.C., 1995. Surface area development of sewage sludge during pyrolysis. Fuel 74, 344–348.
Lu, L., Wenbin, J., Pei, X., 2017. Comparative study on pharmaceuticals adsorption in reclaimed water desalination concentrate using biochar: impact of salts and organic matter. Sci. Total Environ. 601–602, 857–864.
Lu, Q., Zhang, Z.B., Yang, X.C., Dong, C.Q., Zhu, X.F., 2013. Catalytic fast pyrolysis of biomass impregnated with K_3PO_4 to produce phenolic compounds: analytical Py-GC/MS study. J. Anal. Appl. Pyrolysis 104, 139–145.
Lu, X., Flora, J.R.V., Berge, N.D., 2014. Influence of process water quality on hydrothermal carbonization of cellulose. Bioresour. Technol. 154, 229–239.
Luque, R., Menendez, J.A., Arenillas, A., Cot, J., 2012. Microwave-assisted pyrolysis of biomass feedstocks: the way forward? Energy Environ. Sci. 5, 5481–5488.
Lv, G.J., Wu, S.B., Lou, R., 2010. Characteristics of corn stalk hemicellulose pyrolysis in a tubular reactor. Bioresources 5, 2051–2062.
Lv, P.M., Xiong, Z.H., Chang, J., Wu, C.Z., Chen, Y., Zhu, J.X., 2004. An experimental study on biomass air–steam gasification in a fluidized bed. Bioresour. Technol. 95, 95–101.
Ma, Y., Liu, W.J., Zhang, N., Li, Y.S., Jiang, H., Sheng, G.P., 2014. Polyethylenimine modified biochar adsorbent for hexavalent chromium removal from the aqueous solution. Bioresour. Technol. 169, 403–408.
Mahmoud, D.K., Salleh, M.A.M., Karim, W.A.W.A., Idris, A., Abidin, Z.Z., 2012. Batch adsorption of basic dye using acid treated kenaf fibre char: equilibrium, kinetic and thermodynamic studies. Chem. Eng. J. 181–182, 449–457.
Mamleev, V., Bourbigot, S., Le Bras, M., Yvon, J., 2009. The facts and hypotheses relating to the phenomenological model of cellulose pyrolysis: interdependence of the steps. J. Anal. Appl. Pyrolysis 84, 1–17.
Manon, V., Jan, B., Anke, B., Bart, J., Raf, D., 2010. Fundamentals, kinetics and endothermicity of the biomass pyrolysis reaction. Renew. Energy 35, 232–242.

Marion, C., Jan Erns, J., Stephen, D., Thomas, H., Johann, G., Johannes, K., 2013. Impact of the lignocellulosic material on fast pyrolysis yields and product quality. Bioresour. Technol. 150, 129–138.
Martin, P., Barbora, M.R., Vladimir, F., Miroslav, H., Lucia, R., Richard, S., Gerhard, S., 2017. Sorption separation of cobalt and cadmium by straw-derived biochar: a radiometric study. J. Radioanal. Nucl. Chem. 311, 85–97.
Matthew, E., Bidhya, K., Charles, U.P., Dinesh, M., Todd, M., 2015. Sorptive removal of salicylic acid and ibuprofen from aqueous solutions using pine wood fast pyrolysis biochar. Chem. Eng. J. 265, 219–227.
Matthew, W.S., Brennan, P., Greg, H., Louis, S., Manuel, G.P., 2017. Chemical and morphological evaluation of chars produced from primary biomass constituents: cellulose, xylan, and lignin. Biomass Bioenergy 104, 17–35.
McGrath, T.E., Chan, W.G., Hajaligol, M.R., 2003. Low temperature mechanism for the formation of polycyclic aromatic hydrocarbons from the pyrolys is of cellulose. J. Anal. Appl. Pyrolysis 66, 51–70.
Meyer, S., Glaser, B., Quicker, P., 2011. Technical, economical, and climate-related aspects of biochar production technologies: a literature review. Environ. Sci. Technol. 45, 9473–9483.
Michal, K., Isabel, H., Thomas, D.B., Barbara, C., Jadwiga, S.Z., Patryk, O., 2017. Activated biochars reduce the exposure of polycyclic aromatic hydrocarbons in industrially contaminated soils. Chem. Eng. J. 310, 33–40.
Mohamed, B.A., Soo, C., Ellis, N., Bi, X., 2016a. Bioresource Technology Microwave assisted catalytic pyrolysis of switch grass for improving bio-oil and biochar properties. Bioresour. Technol. 201, 121–132.
Mohamed, E.M., Gehan, M.N., Nabila, M.E.M., Heba, I.B., Sandeep, K., Tarek, M.A.F., 2016b. Kinetics, isotherm, and thermodynamic studies of the adsorption of reactive red 195 A dye from water by modified Switchgrass Biochar adsorbent. J. Ind. Eng. Chem. 37, 156–167.
Mohammad, B.A., John, L.Z., Huu, H.N., Wenshan, G., 2016. Insight into biochar properties and its cost analysis, Insight into biochar properties and its cost analysis. Biomass Bioenergy 84, 76–86.
Mohan, D., Pittman Jr., C.U., Steele, P.H., 2006. Pyrolysis of wood/biomass for bio-oil: critical review. Energy Fuels 20, 848–889.
Mohanty, P., Nanda, S., Pant, K.K., Naik, S., Kozinski, J.A., Dalai, A.K., 2013. Evaluation of the physiochemical development of biochars obtained from pyrolysis of wheat straw, timothy grass and pinewood: effects of heating rate. J. Anal. Appl. Pyrolysis 104, 485–493.
Morf, P., Hasler, P., Nussbaumer, T., 2002. Mechanisms and kinetics of homogeneous secondary reactions of tar from continuous pyrolysis of wood chips. Fuel. 81, 843–853.
Motasemi, F., Afzal, M.T., 2013. A review on the microwave-assisted pyrolysis technique. Renew. Sust. Energy Rev. 28, 317–330.
Mubarik, S., Saeed, A., Athar, M.M., Iqbal, M., 2016. Characterization and mechanism of the adsorptive removal of 2,4,6-trichlorophenol by biochar prepared from sugarcane baggase. J. Ind. Eng. Chem. 33, 115–121.
Mui, E.L.K., Cheung, W.H., Valix, M., McKay, G., 2010. Dye adsorption onto char from bamboo. J. Hazard. Mater. 177, 1001–1005.
Mukherjee, A., Lal, R., Zimmerman, A.R., 2014. Effects of biochar and other amendments on the physical properties and greenhouse gas emissions of an artificially degraded soil. Sci. Total Environ. 487, 26–36.
Nabais, J.M.V., Nunes, P., Carrott, P.J.M., Carrott, M.M.L.R., Garcia, A.M., Diez, M.A.D., 2008. Production of activated carbons from coffee endocarp by CO_2 and steam activation. Fuel Process. Technol. 89, 262–268.
Nabajit, D.C., Rahul, S., Chutia, T., Bhaskar, R.K., 2014. Pyrolysis of jute dust: effect of reaction parameters and analysis of products. J. Mater. Cycles Waste. 16, 449–459.
Nan, Z., Honggang, C., Junting, X., Denghui, Y., Zhi, Z., Yun, T., Xiangyang, L., 2017a. Biochars with excellent Pb(II) adsorption property produced from fresh and dehydrated banana peels via hydrothermal carbonization. Bioresour. Technol. 232, 204–210.
Nan, Z., Chuanfang, Z., Yizhong, L., Weifang, Z., Yuguo, D., Zhengping, H., Jing, Z., 2017b. Adsorption and coadsorption mechanisms of Cr(VI) and organic contaminants on H_3PO_4 treated biochar. Chemosphere 186, 422–429.
Neves, D., Thunman, H., Matos, A., Luis, T., Alberto, G.B., 2011. Characterization and prediction of biomass pyrolysis products. Prog. Energy Combust. Sci. 37, 611–630.
Noraini, M.N., Abdullah, E.C., Othman, R., Mubarak, N.M., 2016. Single-route synthesis of magnetic biochar from sugarcane bagasse by microwave-assisted pyrolysis. Mater. Lett. 184, 315–319.
Nzihou, A., Stanmore, B., Sharrock, P., 2013. A review of catalysts for the gasification of biomass char, with some reference to. Coal. Energy 58, 305–317.
Ok, Y.S., Chang, S.X., Gao, B., Chung, H.J., 2015. SMART biochar technology—a shifting paradigm towards advanced materials and healthcare research. Environ. Technol. Innov. 4, 206–209.
Park, H.J., Park, Y.K., Kim, J.S., 2008. Influence of reaction conditions and the char separation system on the production of bio-oil from radiata pine sawdust by fast pyrolysis. Fuel Process Technol. 89, 797–802.
Park, J.H., Ok, Y.S., Kim, S.H., Cho, J.S., Heo, J.S., Delaune, R.D., Seo, D.C., 2015. Evaluation of phosphorus adsorption capacity of sesame straw biochar on aqueous solution: influence of activation methods and pyrolysis temperatures. Environ. Geochem. Health 37, 969–983.
Pehlivan, E., Ozbay, N., Yargic, A.S., Sahin, R.Z., 2017. Production and characterization of chars fromcherrypulpviapyrolysis. J. Environ. Manage. 203, 1017–1025.
Pellera, F.M., Giannis, A., Kalderis, D., Anastasiadou, K., Stegmann, R., Wang, J.Y., Gidarakos, E., 2012. Adsorption of Cu(II) ions from aqueous solutions on biochars prepared from agricultural by-products. J. Environ. Manage. 96, 35–42.
Peng, P., Yin Hai, L., Xiao Mei, W., 2016. Adsorption behavior and mechanism of pentachlorophenol on reed biochars: pH effect, pyrolysis temperature, hydrochloric acid treatment and isotherms. Ecol. Chem. Eng. S 90, 225–233.
Peterson, A.A., Vogel, F., Lachance, R.P., Forling, M., Antal, J., Micheal, W.T., 2008. Thermochemical biofuel production in hydrothermal media: a review of sub- and supercritical water technologies. Energy Environ. Sci. 1, 32–65.
Pimchuai, A., Dutta, A., Basu, P., 2010. Torrefaction of agriculture residue to enhance combustible properties. Energy Fuels 24, 4638–4645.
Pu, Y., Zhang, D., Singh, P.M., Ragauskas, A.J., 2008. The new forestry biofuels sector. Biofuel. Bioprod. Bior. 2, 58–73.
Puja, K., Uzma, D., Rout, P.K., Vinit, Y., Shilpi, J., 2013. Plant refuses driven biochar: alication as metal adsorbent from acidic solutions. Arabian J. Chem. 10, S3054–S3063.
Qian, K., Kumar, A., Zhang, H., Bellmer, D., Huhnke, R., 2015. Recent advances in utilization of biochar. Renew. Sust. Energ Rev. 42, 1055–1064.
Qian, L., Zhang, W., Yan, J., Han, L., Gao, W., Liu, R., Chen, M., 2016. Effective removal of heavy metal by biochar colloids under different pyrolysis temperatures. Bioresour. Technol. 206, 217–224.
Rajapaksha, A.U., Vithanage, M., Ahmad, M., Seo, D.C., Cho, J.S., Lee, S.E., Lee, S.S., Ok, Y.S., 2015. Enhanced sulfamethazine removal by steam-activated invasive plant-derived biochar. J. Hazard. Mater. 290, 43–50.
Rajapaksha, A.U., Vithanage, M., Lee, S.S., Seo, D.C., Tsang, D.C.W., Ok, Y.S., 2016. Steam activation of biochars facilitates kinetics and pH-resilience of sulfamethazine sorption. J. Soils Sediments 16, 889–895.
Rakesh, K.G., Mukul, D., Parashu, K., Zhengrong, G., Qi, H.F., 2015. Biochar activated by oxygen plasma for super capacitors. J. Power Sources 274, 1300–1305.
Rangabhashiyam, S., Suganya, E., Selvaraju, N., Lity, A.V., 2014a. Significance of exploiting non-living biomaterials for the biosorption of wastewater pollutants. World J. Microbiol. Biotechnol. 30, 1669–1689.
Rangabhashiyam, S., Anu, N., Giri Nandagopal, M.S., Selvaraju, N., 2014b. Relevance of isotherm models in biosorption of pollutants by agricultural byproducts. J. Environ. Chem. Eng. 2, 398–414.
Rangabhashiyam, S., Balasubramanian, P., 2018. Adsorption behaviors of hazardous methylene blue and hexavalent chromium on novel materials derived from *Pterospermum acerifolium* shells. J. Mol. Liq. 254, 433–445.
Rangabhashiyam, S., Anu, N., Selvaraju, N., 2013. Sequestration of dye from textile industry wastewater using agricultural waste products as adsorbents. J. Environ. Chem. Eng. 1, 629–641.
Rangabhashiyam, S., Balasubramanian, P., 2016. Lignocellulosic biosorbents for the removal of hexavalent chromium from aqueous solutions: a review. J. Environ. Biotech. Res. 5, 39–46.
Rangabhashiyam, S., Balasubramanian, P., 2017. Dye Removal Prospectives Using Diverse Adsorbents. Lap Lambert Academic Publishing GmbH and Co. KG, Germany.
Rangabhashiyam, S., Selvaraju, N., 2015a. Adsorptive remediation of hexavalent chromium from synthetic wastewater by a natural and $ZnCl_2$ activated *Sterculia guttata* shell. J. Mol. Liq. 207, 39–49.
Rangabhashiyam, S., Selvaraju, N., 2015b. Efficacy of unmodified and chemically modified *Swietenia mahagoni* shells for the removal of hexavalent chromium from simulated wastewater. J. Mol. Liq. 209, 487–497.
Reddy, D.H.K., Lee, S., 2014. Magnetic biochar composite: facile synthesis, characterization, and alication for heavy metal removal. Colloids Surf. A Physicochem. Eng. Asp. 454, 96–103.
Reddy, K., Xie, T., Dastgheibi, S., 2014. Evaluation of biochar as a potential filter media for the removal of mixed contaminants from urban storm water runoff. J. Environ. Eng. New York (New York) 140, 04014043.
Regmi, P., Moscoso, J.L.G., Kumar, S., Cao, X., Mao, J., Schafran, G., 2012. Removal of copper and cadmium from aqueous solution using switchgrass biochar produced via hydrothermal carbonization process. J. Environ. Manage. 109, 61–69.
Reguyal, F., Sarmah, A.K., Gao, W., 2017. Synthesis of magnetic biochar from pine sawdust via oxidative hydrolysis of $FeCl_2$ for the removal sulfamethoxazole from aqueous solution. J. Hazard. Mater. 321, 868–878.
Ricardo, C., G, Margarida., N, Catarina., M, Benilde., 2017. Impact of torrefaction and low-temperature carbonization on the properties of biomass wastes from *Arundo donax* L. And *Phoenix canariensis*. Bioresour. Technol. 223, 210–218.
Roberts, K.G., Gloy, B.A., Joseph, S., Scott, N.R., Lehmann, J., 2010. Life cycle assessment of biochar systems: estimating the energetic, economic, and climate change potential. Environ. Sci. Technol. 44, 827–833.
Roman, S., Nabais, J.M.V., Laginhas, C., Ledesma, B., Gonzalez, J.F., 2012. Hydrothermal carbonization as an effective way of densifying the energy content of biomass. Fuel Process. Technol. 103, 78–83.
Ros, A., Lillo-Rodenas, M.A., Fuente, E., Montes-Moran, M.A., Martina, M.J., Linares-Solano, A., 2006. High surface area materials prepared from sewage sludge-based precursors. Chemosphere 65, 132–140.
Rousset, P., Aguiar, C., Labbe, N., Commandre, J., 2011. Enhancing the combustible properties of bamboo by torrefaction. Bioresour. Technol. 102, 8225–8231.
Rutherford, D.W., Wershaw, R.L., Rostad, C.E., Kelly, C.N., 2012. Effect of formation conditions on biochars: compositional and structural properties of cellulose, lignin, and pine biochars. Biomass Bioenergy 46, 693–701.
Saba, Y., Amirhossein, M., Nasiman, B.S., Sara, Y., 2017. Sorption properties optimization of agricultural wastes-derived biochars using response surface methodology. Process Saf. Envirol. Prot. 109, 509–519.
Sabio, E., Alvarez-Murillo, A., Roman, S., Ledesma, B., 2016. Conversion of tomato-peel waste into solid fuel by hydrothermal carbonization: influence of the processing variables. Waste Manag. 47, 122–132.
Sandip, M., Kaustav, A., Kumar, S., Krishna, S., Rachana, D.C., Gulshan, M., Gopinath, H., 2017. Optimizing ranitidine hydrochloride uptake of Parthenium hysterophorus derived N-biochar through response surface methodology and artificial neural network. Process Saf. Environ. Prot. 107, 388–401.

Sandip, M., Kiran, B., Kaustav, A., Gopinath, H., 2016. Biosorptive uptake of ibuprofen by steam activated biochar derived from mung bean husk: equilibrium, kinetics, thermodynamics, modeling and eco-toxicological studies. J. Environ. Manage. 182, 581–594.
Sara, D., Tushar, K.S., Chi, P., 2017. Synthesis and characterization of slow pyrolysis pine cone bio-char in the removal of organic and inorganic pollutants from aqueous solution by adsorption: kinetic, equilibrium, mechanism and thermodynamic. Bioresour. Technol. 246, 76–81.
Shaaban, A., Se, S.M., Dimin, M.F., Juoi, J.M., Mohd Husin, M.H., Mitan, M.M., 2014. Influence of heating temperature and holding time on biochars derived from rubber wood sawdust via slow pyrolysis. J. Anal. Appl. Pyrolysis 107, 31–39.
Shan, D., Deng, S., Zhao, T., Wang, B., Wang, Y., Huang, J., Yu, G., Winglee, J., Wiesner, M.R., 2016. Preparation of ultrafine magnetic biochar and activated carbon for pharmaceutical adsorption and subsequent degradation by ball milling. J. Hazard. Mater. 305, 156–163.
Shang, J.G., Kong, X.R., He, L.L., Li, W.H., Liao, Q.J.H., 2016. Low-cost biochar derived from herbal residue: characterization and alication for ciprofloxacin adsorption. Int. J. Environ. Sci. Technol. (Tehran) 13, 2449–2458.
Sharma, R.K., Wooten, J.B., Baliga, V.L., Lin, X.H., Chan, W.G., Hajaligol, M.R., 2004. Characterization of chars from pyrolysis of lignin. Fuel 83, 1469–1482.
Shasha, J., Longbin, H., Tuan, A.H.N., Yong, S.O., Victor, R., Hong, Y., Dongke, Z., 2016. Copper and zinc adsorption by softwood and hardwood biochars under elevated sulphate-induced salinity and acidic pH conditions. Chemosphere 142, 64–71.
Sherif, M.T., Mohamed, E.A., Ashraf, E.E., Mohamed, Y.E., 2014. Adsorption of 15 different pesticides on untreated and phosphoric acid treated biochar and charcoal from water. J. Environ. Chem. Eng. 2, 2013–2025.
Shungang, W., Zulin, H., Lei, S., Xue, B., Lu, L., 2016. Biosorption of nitroimidazole antibiotics onto chemically modified porous biochar prepared by experimental design: kinetics, thermodynamics, and equilibrium analysis. Process Saf. Envirol. Prot. 104, 422–435.
Shurong, W., Gongxin, D., Haiping, Y., Zhongyang, L., 2017. Lignocellulosic biomass pyrolysis mechanism: a state-of-the-art review. Prog. Energy Combust. Sci. 62, 33–86.
Sohi, S.P., Krull, E., Lopez-Capel, E., Bol, R., 2010. A review of biochar and its use and function in soil. In: Sparks, D.L. (Ed.), Advances in Agronomy. Academic Press, Burlington, pp. 47–82.
Song, Z., Lian, F., Yu, Z., Zhu, L., Xing, B., Qiu, W., 2014. Synthesis and characterization of a novel MnOx-loaded biochar and its adsorption properties for Cu^{2+} in aqueous solution. Chem. Eng. J. 242, 36–42.
Sonil, N., Javeed, M., Sivamohan, N.R., Janusz, A.K., Ajay, K.D., 2014. Pathways of lignocellulosic biomass conversion to renewable fuels. Biomass Conv. Bioref. 4, 157–191.
Stefanidis, S.D., Kalogiannis, K.G., Iliopoulou, E.F., Michailof, C.M., Pilavachi, P.A., Laas, A.A., 2014. A study of lignocellulosic biomass pyrolysis via the pyrolysis of cellulose, hemicellulose and lignin. J. Anal. Appl. Pyrolysis 105, 143–150.
Sun, L., Chen, D., Wan, S., Yu, Z., 2017. Adsorption studies of dimetridazole and metronidazole onto biochar derived from sugarcane bagasse: kinetic, equilibrium, and mechanisms. J. Polym. Environ. 26 (Feb. (2)), 765–777. https://doi.org/10.1007/s10924-017-0986-5.
Sun, P., Hui, C., Azim Khan, R., Du, J., Zhang, Q., Zhao, Y.H., 2015. Efficient removal of crystal violet using Fe_3O_4-coated biochar: the role of the Fe_3O_4 nanoparticles and modeling study their adsorption behavior. Sci. Rep. 5, 12638.
Suriapparao, D.V., Vinu, R., 2015. Bio-oil production via catalytic microwave pyrolysis of model municipal solid waste component mixtures. RSC Adv. 5, 57619–57631.
Taba, L.E., Irfan, M.F., Daud, W.A.M.W., Chakrabarti, M.H., 2012. The effect of temperature on various parameters in coal, biomass and CO-gasification: a review. Renew. Sust. Energy Rev. 16, 5584–5596.
Takaya, C.A., Fletcher, L.A., Singh, S., Okwuosa, U.C., Ross, A.B., 2016. Recovery of phosphate with chemically modified biochars. J. Environ. Chem. Eng. 4, 1156–1165.
Tan, X.F., Liu, S.B., Liu, Y.G., Gu, Y.L., Zeng, G.M., Hu, X.J., Wang, X., Liu, S.H., Jiang, L.H., 2017. Biochar as potential sustainable precursors for activated carbon production: multiple applications in environmental protection and energy storage. Bioresour. Technol. 227, 359–372.
Tao, K., Vladimir, S., Tim, J.E., 2016. Lignocellulosic biomass pyrolysis : A review of product properties and effects of pyrolysis parameters. Renew. Sust. Energy Rev. 57, 1126–1140.
Tarek, M.A.F., Mohamed, E.M., Somia, B.A., Matthew, D.H., James, W.L., Sandeep, K., 2015. Biochar from woody biomass for removing metal contaminants and carbon sequestration. J. Ind Eng. Chem. 22, 103–109.
Thines, K.R., Abdullah, E.C., Mubarak, N.M., 2017. Effect of process parameters for production of microporous magnetic biochar derived from agriculture waste biomass. Microporous Mesoporous Mater. 253, 29–39.
Thomsen, T., Hauggaard-Nielsen, H., Bruun, E.W., Ahrenfeldt, J., 2011. The Potential of Pyrolysis Technology in Climate Change Mitigation – Influence of Process Design and – Parameters, Simulated in SuprPro Designer Software. Roskilde: Technical University of Denmark.
Tong, C., Jiane, Z., Fenglin, L., 2017. Performance and mechanism for cadmium and lead adsorption from water and soil by corn straw biochar. Front. Environ. Sci. Eng. China 11, 15–22.
Tong, X.J., Li, J.Y., Yuan, J.H., Xu, R.K., 2011. Adsorption of Cu(II) by biochars generated from three crop straws. Chem. Eng. J. 172, 828–834.
Trakal, L., Veselska, V., Safarík, I., Vitkova, M., Číhalova, S., Komarek, M., 2016. Lead and cadmium sorption mechanisms on magnetically modified biochars. Bioresour. Technol. 203, 318–324.
Tripathi, M., Sahu, J.N., Ganesan, P., 2016. Effect of process parameters on production of biochar from biomass waste through pyrolysis: a review. Renew. Sust. Energy Rev. 55, 467–481.
Uchimiya, M., Bannon, D.I., Wartelle, L.H., Lima, I.M., Klasson, K.T., 2012. Lead retention by broiler litter biochars in small arms range soil: impact of pyrolysis temperature. J. Agric. Food Chem. 60, 5035–5044.
Uchimiya, M., Chang, S., Klasson, K.T., 2011. Screening biochars for heavy metal retention in soil: role of oxygen functional groups. J. Hazard. Mater. 190, 432–441.
Uchimiya, M., Lima, I.M., Klasson, K.T., Chang, S.C., Wartelle, L.H., Rodgers, J.E., 2010. Immobilization of heavy metal ions (Cu-II, Cd-II, Ni-II, and Pb-II) by broiler litter-derived biochars in water and soil. J. Agric. Food Chem. 58, 5538–5544.
Uddin, M.N., Daud, W.M.A.W., Abbas, H.F., 2014. Effects of pyrolysis parameters on hydrogen formations from biomass: a review. RSC Adv. 4, 10467–10490.
Unai, I.V., Irene, S., Lorena, Z., Jose, L.A., 2016. Preparation of a porous biochar from the acid activation of pork bones. Food Bioprod. Process. 98, 341–353.
Vaibhav, D., Thallada, B., 2017. A comprehensive review on the pyrolysis of lignocellulosic biomass. Renew. Energy 129, 695–716.
Van, V.M., Baeyens, J., Brems, A., Bart, J., Raf, D., 2010. Fundamentals, kinetics and endothermicity of the biomass pyrolysis reaction. Renew. Energy 35, 232–242.
Vinke, P., Van der Eijk, M., Verbree, M., Voskamp, A., Van Bekkum, H., 1994. Modification of the surfaces of a gas activated carbon and a chemically activated carbon with nitric acid, hypochlorite, and ammonia. Carbon 32, 675–686.
Vithanage, M., Herath, I., Joseph, S., Bundschuh, J., Bolan, N., Ok, Y.S., Kirkham, M.B., Rinklebe, J., 2017. Interaction of arsenic with biochar in soil and water: A critical review. Carbon 113, 219–230.
Vithanage, M., Rajapaksha, A.U., Ahmad, M., Uchimiya, M., Dou, X., Alessi, D.S., Ok, Y.S., 2015a. Mechanisms of antimony adsorption onto soybean stover derived biochar in aqueous solutions. J. Environ. Manage. 151, 443–449.
Vithanage, M., Rajapaksha, A.U., Dou, X., Bolan, N.S., Yang, J.E., Ok, Y.S., 2013. Surface complexation modeling and spectroscopic evidence of antimony adsorption on iron-oxide-rich red earth soils. J. Colloid Interface Sci. 406, 217–224.
Vithanage, M., Rajapaksha, A.U., Zhang, M., Thiele-Bruhn, S., Lee, S.S., Ok, Y.S., 2015b. Acid-activated biochar increased sulfamethazine retention in soils. Environ. Sci. Pollut. Res. 22, 2175–2186.
Vladimir, F., Martin, P., Juraj, L., Gerhard, S., Wolfgang, F.H., Alena, P., 2015. Utilization of biochar sorbents for Cd^{2+}, Zn^{2+}, and Cu^{2+} ions separation from aqueous solutions: comparative study. Environ. Monit. Assess. 187, 4093–4111.
Volesky, B., 1994. Advances in biosorption of metal: selection of biomass types. FEMS Microbiol. Rev. 14, 291–302.
Wang, B.Y., Li, C.P., Liang, H., 2013. Bioleaching of heavy metal from woody biochar using *Acidithiobacillus ferrooxidans* and activation for adsorption. Bioresour. Technol. 146, 803–806.
Wang, M.C., Sheng, G.D., Qiu, Y.P., 2015a. A novel manganese-oxide/biochar composite for efficient removal of lead(II) from aqueous solutions. Int. J. Environ. Sci. Technol. (Tehran) 12, 1719–1726.
Wang, S., Gao, B., Li, Y., Mosa, A., Zimmerman, A.R., Ma, L.Q., Harris, W.G., Migliaccio, K.W., 2015b. Manganese oxide-modified biochars: preparation, characterization, and sorption of arsenate and lead. Bioresour. Technol. 181, 13–17.
Wang, S., Gao, B., Zimmerman, A.R., Li, Y., Ma, L., Harris, W.G., Migliaccio, K.W., 2015c. Removal of arsenic by magnetic biochar prepared from pinewood and natural hematite. Bioresour. Technol. 175, 391–395.
Wang, X.S., Chen, L.F., Li, F.Y., Chen, K.L., Wan, W.Y., Tang, Y.J., 2010. Removal of Cr (VI) with wheat-residue derived black carbon: reaction mechanism and adsorption performance. J. Hazard. Mater. 175, 816–822.
Wang, Z., Pecha, B., Westerhof, R.J.M., Kersten, S.R.A., Li, C.Z., McDonald, A.G., Garcia-Perez, M., 2014. Effect of cellulose crystallinity on solid/liquid phase reactions responsible for the formation of carbonaceous residues during pyrolysis. Ind. Eng. Chem. Res. 53, 2940–2955.
Wei, L., Xu, S., Zhang, L., Zhang, H., Liu, C., Zhu, H., Liu, S., 2006. Characteristics of fast pyrolysis of biomass in a free fall reactor. Fuel Process. Technol. 87, 863–871.
Wei, Z., Mingxin, G., Teresa, C., Douglas, N.B., Nandakishore, R., 2010. Sorption properties of greenwaste biochar for two triazine pesticides. J. Hazard. Mater. 181, 121–126.
Wilk, M., Magdziarz, A., Kalemba, I., 2015. Characterization of renewable fuels' torrefaction process with different instrumental techniques. Energy 87, 259–269.
Wooten, J.B., Seeman, J.I., Hajaligol, M.R., 2004. Observation and characterization of cellulose pyrolysis intermediates by C-13 CPMAS NMR. A new mechanistic model. Energy Fuel 18, 1–15.
Xiao, F., Pignatello, J.J., 2015. Interactions of triazine herbicides with biochar: steric and electronic effects. Water Res. 80, 179–188.
Xiaoling, D., Lena, Q.M., Yuncong, L., 2011. Characteristics and mechanisms of hexavalent chromium removal by biochar from sugar beet tailing. J. Hazard. Mater. 190, 909–915.
Xin, S.Z., Yang, H.P., Chen, Y.Q., Wang, X.H., Chen, H.P., 2013. Assessment of pyrolysis polygeneration of biomass based on major components: product characterization and elucidation of degradation pathways. Fuel 113, 266–273.
Xin, S.Z., Yang, H.P., Chen, Y.Q., Yang, M.F., Chen, L., Wang, X.H., Chen, H.P., 2015. Chemical structure evolution of char during the pyrolysis of cellulose. J. Anal. Appl. Pyrolysis 116, 263–271.
Xingfeng, Z., Xuehong, Z., Zhigang, C., 2017. Biosorption of Cr(VI) from aqueous solution by biochar derived from the leaf of *Leersia hexandra* Swartz. Environ. Earth Sci. 76, 67–73.
Xinsheng, L., Zhe, Z., Pengxin, Z., Yani, L., Guofu, M., Ziqiang, L., 2015. Synergic adsorption of acid blue 80 and heavy metal ions (Cu^{2+}/Ni^{2+}) onto activated carbon and its mechanisms. J. Ind. Eng. Chem. 27, 164–174.
Xu, Z., Xuezhen, W., Hai, Z., Haiming, W., 2017. Enhanced nitrogen removal of low C/N domestic wastewater using a biochar-amended aerated vertical flow constructed wetland. Bioresour. Technol. 241, 269–275.
Xu, R.K., Xiao, S.C., Yuan, J.H., Zhao, A.Z., 2011. Adsorption of methyl violet from

aqueous solutions by the biochars derived from crop residues. Bioresour. Technol. 102, 10293–10298.
Xu, Y., Chen, B., 2014. Organic carbon and inorganic silicon speciation in rice-bran derived biochars affect its capacity to adsorb cadmium in solution. J. Soils Sediments 15, 60–70.
Xuan, L., Yang, Z., Zifu, L., Rui, F., Yaozhong, Z., 2014. Characterization of corncob-derived biochar and pyrolysis kinetics in comparison with corn stalk and sawdust. Bioresour. Technol. 170, 76–82.
Xue, Y.W., Gao, B., Yao, Y., Inyang, M., Zhang, M., Zimmerman, A.R., Ro, K.S., 2012. Hydrogen peroxide modification enhances the ability of biochar (hydrochar) produced from hydrothermal carbonization of peanut hull to remove aqueous heavy metals: batch and column tests. Chem. Eng. J. 200, 673–680.
Xuefei, C., Linxin, Z., Xinwen, P., Shaoni, S., Shouming, L., Shijie, L., Runcang, S., 2014. Comparative study of the pyrolysis of lignocellulose and its major components: characterization and overall distribution of their biochars and volatiles. Bioresour. Technol. 155, 21–27.
Yakkala, K., Yu, M.R., Roh, H., Yang, J.K., Chang, Y.Y., 2013. Buffalo weed (*Ambrosia trifida*L. var. trifida) biochar for cadmium(II) and lead(II) adsorption in single and mixed system. Desalin. Water Treat. 51, 7732–7745.
Yan, L., Kong, L., Qu, Z., Li, L., Shen, G., 2014. Magnetic biochar decorated with ZnS nanocrystals for Pb(II) removal. ACS Sustain. Chem. Eng. 3, 125–132.
Yan, X., Yunguo, L., Shaobo, L., Xiaofei, T., Guangming, Z., Wei, Z., Yang, D., Weicheng, C., Bohong, Z., 2016. Enhanced adsorption of methylene blue by citric acid modification of biochar derived from water hyacinth (*Eichornia crassipes*). Environ. Sci. Pollut. Res. Int. 23, 23606–23618.
Yanan, C., Baoshan, Y., Ziheng, S., Hui, W., Fei, H., Xuemei, H., 2016. Wheat straw biochar amendments on the removal of polycyclic aromatic hydrocarbons (PAHs) in contaminated soil. Ecotoxicol. Environ. Saf. 130, 248–255.
Yanfang, F., Dionysios, D.D., Yonghong, W., Hui, Z., Lihong, X., Shiying, H., Linzhang, Y., 2013. Adsorption of dyestuff from aqueous solutions through oxalic acid-modified swede rape straw: adsorption process and disposal methodology of depleted bioadsorbents. Bioresour. Technol. 138, 191–197.
Yang, H.P., Yan, R., Chen, H.P., Lee, D.H., Zheng, C.G., 2007. Characteristics of hemicellulose, cellulose and lignin pyrolysis. Fuel 86, 1781–1788.
Yang, Y., Lin, X., Wei, B., Zhao, Y., Wang, J., 2013. Evaluation of adsorption potential of bamboo biochar for metal-complex dye: equilibrium, kinetics and artificial neural network modeling. Int. J. Environ. Sci. Technol. (Tehran) 2014 (11), 1093–1100.
Yang, Z., Xiong, S., Wang, B., Li, Q., Yang, W., 2013. Cr(III) adsorption by sugarcane pulp residue and biochar. J. Cent. South. Univ. 20, 1319–1325.
Yanxue, H., Akwasi, A.B., Phoebe, X.Q., Isabel, M.L., Jianmin, C., 2013. Heavy metal and phenol adsorptive properties of biochars from pyrolyzed switchgrass and woody biomass in correlation with surface properties. J. Environ. Manage. 118, 196–204.
Yao, Y., Gao, B., Chen, H., Jiang, L., Inyang, M., Zimmerman, A.R., Cao, X., Yang, L., Xue, Y., Li, H., 2012. Adsorption of sulfamethoxazole on biochar and its impact on reclaimed water irrigation. J. Hazard. Mater. 209, 408–413.
Yao, Y., Gao, B., Chen, J., Zhang, M., Inyang, M., Li, Y., Alva, A., Yang, L., 2013. Engineered carbon (biochar) prepared by direct pyrolysis of Mg-accumulated tomato tissues: characterization and phosphate removal potential. Bioresour. Technol. 138, 8–13.
Yorgun, S., Vural, N., Demiral, H., 2009. Preparation of high-surface area activated carbon from Paulownia by $ZnCl_2$ activation. Microporous Mesoporous Mater. 122, 189–194.
Yu, J., Paterson, N., Blamey, J., Millan, M., 2017. Cellulose, xylan and lignin interactions during pyrolysis of lignocellulosic biomass. Fuel 191, 140–149.
Yuan, H., Lu, T., Zhao, D., Huang, H., Noriyuki, K., Chen, Y., 2013. Influence of temperature on product distribution and biochar properties by municipal sludge pyrolysis. J. Mater. Cycles Waste. 15, 357–361.
Yuping, Q., Zhenzhi, Z., Zunlong, Z., Sheng, G.D., 2009. Effectiveness and mechanisms of dye adsorption on a straw-based biochar. Bioresour. Technol. 100, 5348–5351.
Zanzi, R., Sjostrom, K., Bjornbom, E., 1996. Rapid high-temperature pyrolysis of biomass in a free-fall reactor. Fuel. 75, 545–550.
Zhang, F.S., Nriagu, J.O., Itoh, H., 2005. Mercury removal from water using activated carbons derived from organic sewage sludge. Water Res. 39, 389–395.
Zhang, H., Voroney, R.P., Price, G.W., 2015a. Effects of temperature and processing conditions on biochar chemical properties and their influence on soil C and N transformations. Soil Biol. Biochem. 83, 19–28.
Zhang, J., Liu, J., Liu, R., 2015b. Effects of pyrolysis temperature and heating time on biochar obtained from the pyrolysis of straw and lignosulfonate. Bioresour. Technol. 176, 288–291.
Zhang, J., Nolte, M.W., Shanks, B.H., 2014a. Investigation of primary reactions and secondary effects from the pyrolysis of different celluloses. ACS Sustain. Chem. Eng. 2, 2820–2830.
Zhang, J., Wang, Q., 2016. Sustainable mechanisms of biochar derived from brewers' spent grain and sewage sludge for ammonia–nitrogen capture. J. Clean. Prod. 112, 3927–3934.
Zhang, M., Gao, B., 2013. Removal of arsenic, methylene blue, and phosphate by biochar/AlOOH nanocomposite. Chem. Eng. J. 226, 286–292.
Zhang, M., Gao, B., Varnoosfaderani, S., Hebard, A., Yao, Y., Inyang, M., 2013b. Preparation and characterization of a novel magnetic biochar for arsenic removal. Bioresour. Technol. 130, 457–462.
Zhang, M., Gao, B., Yao, Y., Xue, Y., Inyang, M., 2012b. Synthesis, characterization, and environmental implications of graphene-coated biochar. Sci. Total Environ. 435, 567–572.
Zhang, M., Gao, B., Yao, Y., Xue, Y., Inyang, M., 2012a. Synthesis of porous MgO biochar nanocomposites for removal of phosphate and nitrate from aqueous solutions. Chem. Eng. J. 210, 26–32.
Zhang, X., Zhang, S., Yang, H., Shi, T., Chen, Y., Chen, H., 2013a. Influence of NH_3/CO_2 modification on the characteristic of biochar and the CO_2 capture. Bioenerg. Res. 6, 1147–1153.
Zhang, Y.J., Xing, Z.J., Duan, Z.K., Li, M., Wang, Y., 2014b. Effects of steam activation on the pore structure and surface chemistry of activated carbon derived from bamboo waste. Appl. Surf. Sci. 315, 279–286.
Zhantao, H., Badruddeen, S., Wojciech, M., Martin, O., Barbara, B., Hrissi, K.K., David, W., 2015. Magnetite impregnation effects on the sorbent properties of activated carbons and biochars. Water Res. 70, 394–403.
Zheng, H., Wang, Z., Deng, X., Zhao, J., Luo, Y., Novak, J., Herbert, S., Xing, B., 2013. Characteristics and nutrient values of biochars produced from giant reed at different temperatures. Bioresour. Technol. 130, 463–471.
Zhengtao, S., Yiyun, Z., Fei, J., Oliver, M.M., Abir, A.T., 2017. Qualitative and quantitative characterisation of adsorption mechanisms of lead on four biochars. Sci. Total Environ. 609, 1401–1410.
Zhou, Y., Gao, B., Zimmerman, A.R., Chen, H., Zhang, M., Cao, X., 2014. Biochar suorted zerovalent iron for removal of various contaminants from aqueous solutions. Bioresour. Technol. 152, 538–542.
Zhou, Z., Liu, Y., Liu, S., Liu, H., Zeng, G., Tan, X., Yang, C., Ding, Y., Yan, Z., Cai, X., 2017. Sorption performance and mechanisms of arsenic(V) removal by magnetic gelatin-modified biochar. Chem. Eng. J. 314, 223–231.
Zhu, N., Yan, T., Qiao, J., Cao, H., 2016. Adsorption of arsenic, phosphorus and chromium by bismuth impregnated biochar: adsorption mechanism and depleted adsorbent utilization. Chemosphere 164, 32–40.
Zhu, X., Liu, Y., Qian, F., Zhou, C., Zhang, S., Chen, J., 2014. Preparation of magnetic porous carbon from waste hydrochar by simultaneous activation and magnetization for tetracycline removal. Bioresour. Technol. 154, 209–214.
Zhuhong, D., Xin, H., Yongshan, W., Shengsen, W., Bin, G., 2016a. Removal of lead, copper, cadmium, zinc, and nickel from aqueous solutions by alkali-modified biochar: batch and column tests. J. Ind. Eng. Chem. 33, 239–245.
Zhuhong, D., Yongshang, W., Xin, H., Shengsen, W., Andrew, R.Z., Bin, G., 2016b. Sorption of lead and methylene blue onto hickory biochars from different pyrolysis temperatures: importance of physicochemical properties. J. Ind. Eng. Chem. 37, 261–267.